

Large-Scale Evaluation of Open-Set Image Classification Techniques

Halil Bisgin

*Department of Computer Science
University of Michigan-Flint
Flint, MI 48502, USA*

BISGIN@UMICH.EDU

Andres Palechor

Mike Suter

Manuel Günther

*Department of Informatics
University of Zurich
Andreasstrasse 15
8050 Zurich, Switzerland*

ANDRESPALECHOR11@GMAIL.COM

MIKE.MILOW.SUTER@GMAIL.COM

SIEBENKOPF@GOOGLEMAIL.COM

Abstract

The goal for classification is to correctly assign labels to unseen samples. However, most methods misclassify samples with unseen labels and assign them to one of the known classes. Open-Set Classification (OSC) algorithms aim to maximize both closed and open-set recognition capabilities. Recent studies showed the utility of such algorithms on small-scale data sets, but limited experimentation makes it difficult to assess their performances in real-world problems. Here, we provide a comprehensive comparison of various OSC algorithms, including training-based (SoftMax, Garbage, EOS) and post-processing methods (Maximum SoftMax Scores, Maximum Logit Scores, OpenMax, EVM, PROSER), the latter are applied on features from the former. We perform our evaluation on three large-scale protocols that mimic real-world challenges, where we train on known and negative open-set samples, and test on known and unknown instances. Our results show that EOS helps to improve performance of almost all post-processing algorithms. Particularly, OpenMax and PROSER are able to exploit better-trained networks, demonstrating the utility of hybrid models. However, while most algorithms work well on negative test samples – samples of open-set classes seen during training – they tend to perform poorly when tested on samples of previously unseen unknown classes, especially in challenging conditions.

Keywords: open-set classification, large-scale evaluation, image classification, deep learning, reproducible research

1. Introduction

The automated classification of visual objects into several classes has a long history in science. Specifically, categorical classification is trying to discriminate between different categories, such as identifying handwritten digits, traffic signs, birds, or broader categories as provided by the ImageNet data set (Deng et al., 2009). The breakthrough in this image classification task was by introducing convolutional neural networks to perform this task (LeCun et al., 1995; Krizhevsky et al., 2012), which has shown to outperform any traditional method. Nowadays, more modern and deeper network architectures are created to perform

this task (He et al., 2016; Huang et al., 2017; Yuan et al., 2021), which are typically trained on large amounts of data with (variations of) the SoftMax loss.

When during deployment only samples of the learned classes are present, these classifiers perform *closed-set* classification. However, when applying these classifiers in the real world, it cannot be guaranteed that the input always comes from previously seen classes. For example, when a digit classifier is presented with a letter, it will assign one of the ten digits instead (Dhamija et al., 2018). There are several approaches to counter this behavior. One such class of methods is *anomaly* or *out-of-distribution detection*, which will classify whether a certain object is likely to belong to a class unseen during training. Such methods usually perform well when the unknown test data is far away from the known classes, but will typically fail when known and unknown classes are similar. One easy *post-processing* method for anomaly detection is the Maximum SoftMax Score (MSS) approach by Hendrycks and Gimpel (2017), which turns the network outputs into probabilities through SoftMax activation and thresholds the maximum achieved probability. An alternative is Maximum Logit Score (MLS) approach from Hendrycks et al. (2022), which directly employs the network outputs (also known as the *logits*) as confidence scores without relying on SoftMax transformation.

Another class of methods deals with the issue of unknown test samples via Open-Set Classification (OSC). Here, a classifier that is able to classify the known classes is augmented with the possibility to reject unknown samples. While early OSC approaches, such as OpenMax (Bendale and Boult, 2016) and Extreme Value Machine (EVM) (Rudd et al., 2017) mainly rely on output of trained networks in the context of deep learning, later methods try to modify the network such that it has an option to reject unknown samples. One typical example for the latter group is introducing an additional *garbage class* as an output to the network, an approach that arose early (Matan et al., 1990), was applied in many object detection methods (Ren et al., 2015; Redmon et al., 2016; Jiang and Learned-Miller, 2017; Zhao et al., 2019), and now has become widely adopted in open-set classification (Ge et al., 2017; Neal et al., 2018; Zhou et al., 2021; Chen et al., 2022). A different approach was introduced by Dhamija et al. (2018) who proposed the Entropic Open-Set (EOS) loss and the Objectosphere loss to avoid the network to produce any large probability for unknown samples, without needing to model the probability of unknown explicitly.

All these types of network-based OSC algorithms require training on *negative* data, also termed *known unknown* data in the literature, *i. e.* data that does not belong to any of the known classes. Some approaches made use of real negative samples from different data sets (Dhamija et al., 2018; Palechor et al., 2023), while other researchers tried to build such negative samples by modifying or combining known samples (Zhou et al., 2021; Wilson et al., 2023) or by artificially generating negative samples (Ge et al., 2017). For example, the PROSER algorithm (Zhou et al., 2021) performs manifold mixup of middle-level features of two samples from different known classes (Verma et al., 2019) to build negative samples.

Many evaluation data sets in the open-set classification task are small, with small numbers of classes, but an abundance of samples per class. For example, many researchers in open-set image classification make use of (various combinations of) MNIST (LeCun et al., 1998), CIFAR-10/100 (Krizhevsky and Hinton, 2009), SVHN (Netzer et al., 2011), Fashion-MNIST (Xiao et al., 2017) or Tiny ImageNet challenge (Le and Yang, 2015), but other small-scale data sets are also used. Some researchers even include random noise with different distributions as unknown samples (Liang et al., 2017), which clearly does not provide

any insight on how algorithms react to samples of unknown classes. Generally, these data sets have been introduced for closed-set image classification, and different random and non-standard evaluation protocols are designed by many researchers. While designing new open-set techniques might be fostered by such small-scale data sets since experimentation is quick, they do not represent realistic views of real-world tasks. The issue with these protocols is that known and unknown classes are typically visually and semantically distinctive and, thus, the task at hand is more related to out-of-distribution detection than on open-set classification. The lack of large-scale evaluations has also been acknowledged in the out-of-distribution detection field, for which lately new evaluation benchmarks have been introduced by Yang et al. (2022), but their proposed OSC benchmark still relies on small-scale data sets.

Additionally, most researchers evaluate their methods with metrics that are not designed to (and, therefore, not able to) evaluate open-set classification realistically.¹ Dhamija et al. (2018, 2019) have designed the Open-Set Classification Rate (OSCR) curve, which treats known and unknown test samples differently and follows the well-known Open-Set ROC curve actively applied in face recognition (Phillips et al., 2011; Grother et al., 2022). The OSCR metric is nowadays widely adopted for open-set classification, but in many publications it is used as a single number (Vaze et al., 2022; Chen et al., 2022) without specifying how exactly this number is computed, so a comparison with these works is not possible – we here assume that they report the Area Under the OSCR curve.

Lately, we have introduced a new open-set image classification challenge (Palechor et al., 2023) based on the ImageNet data set used in the ImageNet Large Scale Visual Recognition Challenges (ILSVRC) (Russakovsky et al., 2015). Using the WordNet hierarchy (Miller, 1998), we designed three different evaluation protocols with varying semantic similarity between known and unknown classes, as can be seen in Figure 1. Additionally, we provide real negative samples to foster research in training OSC methods with them. The variations in semantic similarities, which can be also inferred by following the dashed lines in the same figure, contributed to the difficulty levels of protocols. For instance, in the first protocol, P_1 , known and unknown classes are semantically quite distant from each other while negative classes are close to the known class, which made P_1 easy for open-set and hard for closed-set classification. Protocols P_2 and P_3 are also constructed by following different semantic distances to have richer and more realistic scenarios. While other evaluation protocols on ImageNet exist (Bendale and Boulton, 2016; Vaze et al., 2022) they make use of the total of the ILSVRC 2012 data set as known classes and do not provide negative samples, which disallows to have large shifts between known and unknown classes, limits the algorithms that can be applied to them, and prohibit extensive experimentation through the expensive training on the large data set.

The contributions of this paper are as follows:

- We perform the first large-scale evaluation of several training-based and post-processing methods for open-set classification.
- For the first time in the literature, we combine these orthogonal methods to further improve performance.

1. See Dhamija et al. (2018); Boulton et al. (2019); Wang et al. (2022); Palechor et al. (2023) for a more detailed discussion on drawbacks of existing evaluation techniques.

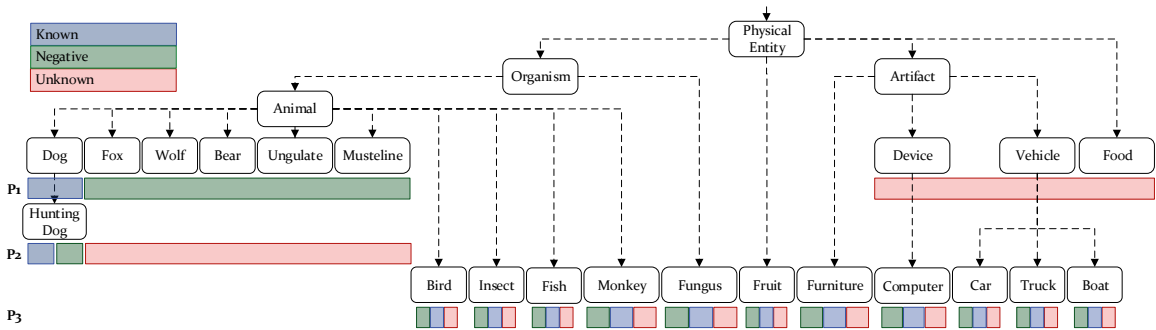


Figure 1: OPEN-SET PROTOCOLS FOR IMAGENET. This figure shows the partition of classes into known, negative and unknown within the three different protocols, P_1 , P_2 , and P_3 . By following the WordNet hierarchy (Miller, 1998) which is shown with the dashed lines indicating an “is-a” relationship, we sample our final classes from the leaf nodes of the intermediate-level superclasses named above the colored bars. The colored bars below indicate that its subclasses are sampled for the same color codes representing knowns, negatives and unknowns. For example, all subclasses of “Dog” are used as known classes in P_1 , while the subclasses of “Hunting Dog” are partitioned into knowns and negatives in P_2 . On the other hand, P_3 has several intermediate nodes that are partitioned into known, negative, and unknown classes. Those partitions also constitute training, validation, and test sets in each protocol. While known and negative classes are available during training and validation, unknown classes only appear in test time. More details on the protocols are provided by Palechor et al. (2023).

- We exploit the evaluation protocols that we previously defined (Palechor et al., 2023) and the evaluation metric designed by Dhamija et al. (2018) to perform a fair and realistic evaluation of the methods.
- We make use of publicly available implementations as far as possible, and re-implement methods when required. We provide all of our implementations and evaluation techniques as open-source package,² hoping to foster more research and more fair and realistic evaluations of open-set classification techniques in the future.

2. Open-Set Classification Taxonomy

As we noted in Section 1, open-set classification approaches can either perform additional training with some adjustments or make use of deep features to correctly classify known samples and identify unknowns in a deep learning framework. These two kinds of approaches lead us to a taxonomy we adopt in this work: (a) *training-based methods* try improving the network by including a reject option into the training procedure of the network directly, and (b) *post-processing methods* use existing features or scores, which are nowadays typically extracted from a pretrained closed-set network, to provide probabilities p_c for all *known* classes $c \in \{1, \dots, K\}$, possibly by learning a secondary classifier.

2. <https://github.com/AIIML-IfI/openset-imagenet-comparison>



Figure 2: PROCESSING WITH DEEP NETWORKS. An image is presented to the backbone network, which extracts deep features $\vec{\varphi}$ that are then processed with a Linear layer to logits \vec{z} , and further with SoftMax to probabilities \vec{y} .

These probabilities can finally be evaluated in open-set metrics, which we define in Section 4.2. Please note that we do not require to compute the probability of the unknown class p_{K+1} . A low probability for the unknown class p_{K+1} does not indicate a high probability for any of the known classes. On the other hand, due to SoftMax requiring that probabilities sum up to 1, a large p_{K+1} probability enforces low probabilities for all known classes. Therefore, p_{K+1} does not add any new information.

2.1 Training-based Methods

A typical processing with deep networks takes place as shown in Figure 2, where images are passed to a backbone network, which is ResNet-50 in our case, and their logits \vec{z} output from a fully-connected layer are turned into probabilities \vec{y} through SoftMax:

$$y_{n,c} = \frac{e^{z_{n,c}}}{\sum_{c'=1}^C e^{z_{n,c'}}}. \quad (1)$$

Based on these, the weighted categorical cross-entropy loss can be computed as:

$$\mathcal{J}_{\text{CCE}} = -\frac{1}{N} \sum_{n=1}^N \sum_{c=1}^C w_c t_{n,c} \log y_{n,c} \quad (2)$$

where N is the number of samples in our data set (note that we utilize batch processing), $t_{n,c}$ is the target label of the n th sample for class c , w_c is a class-weight for class c and $y_{n,c}$ is the confidence of class c for sample n using SoftMax activation.

In our training-based category, we use three variations of this paradigm, which employ SoftMax, Garbage class, and Entropic Open-Set (EOS) loss. These are the same three techniques to train the deep networks as in (Palechor et al., 2023). We solely use categorical cross-entropy loss on top of SoftMax activations (also known as the SoftMax loss) to train our networks. The three different training approaches differ with respect to the targets $t_{n,c}$ and the weights w_c , and how negative samples are handled. A more technical explanation of these methods are given in Section 3.1.

While the largest amount of research in open-set classification tries to artificially generate effective negative samples to train the networks (Ge et al., 2017; Neal et al., 2018; Chen

et al., 2020, 2022), in our evaluation we solely rely on the real negative samples provided in our protocols. For a more detailed analysis of other existing OSC techniques, we refer the reader to Geng et al. (2021).

2.2 Post-processing Methods

Most of the early approaches to open-set classification fall into the category of feature or score post-processing. Bendale and Boulton (2016) introduced the OpenMax method to add a probability of unknown by modeling deep feature distributions. Rudd et al. (2017) introduced the Extreme Value Machine (EVM) to compute a probability of sample inclusion for each of the known classes based on their feature similarities and Günther et al. (2017) showed its extensibility to deep feature space. Günther et al. (2020) implemented a shallow network on top of deep features extracted from a face recognition network to perform open-set face recognition. Recently, Hendrycks and colleagues (Hendrycks and Gimpel, 2017; Hendrycks et al., 2022) indicated that simply thresholding the output of the pretrained network can provide a reasonable option for OSC.

A clear disadvantage of these approaches is that they cannot undo any damage to the feature representation learned by the pretrained network, *e. g.*, when samples from known and unknown classes overlap in deep feature space, neither of them can improve the open-set performance of the network. Therefore, Zhou et al. (2021) have introduced a hybrid approach, the PlaceholderS for Open-SEt Recognition (PROSER), which starts with a pretrained network and adds post-hoc open-set capabilities to that network.

Due to the ease of application or the availability of open source code, our post-processing category includes the following five open-set methods on top of our trained networks for which we provide formal definitions in Section 3.2:

- Maximum SoftMax Score (MSS) uses the SoftMax scores (1) of the networks and serves as the baseline (Hendrycks and Gimpel, 2017).
- Maximum Logit Score (MLS) relies on the logits z_c , *i. e.*, the direct outputs of the network (Hendrycks et al., 2022).
- OpenMax uses logits and deep features to obtain a probability of unknown (Bendale and Boulton, 2016).
- Extreme Value Machine (EVM) exploits deep features to reject unknown samples (Rudd et al., 2017).
- PlaceholderS for Open-SEt Recognition (PROSER) fine-tunes the network and adds outputs for unknown (Zhou et al., 2021).

3. Evaluated Methods

We evaluate two complementary types of open-set methods: training-based and post-processing. Additionally, for the first time in the literature, we try combinations of training-based and post-processing methods. We first train the training-based method to provide features that are able to separate known classes from each other and also from unknown

classes, and we apply post-processing algorithms to further improve the separability. Here, we provide the technical details of all applied algorithms.

3.1 Training-based Methods

The first approach in the training-based category is the plain SoftMax loss (S) that is trained only on samples from the K known classes, since this has been shown to be a strong baseline for out-of-distribution detection algorithms (Hendrycks and Gimpel, 2017; Hendrycks et al., 2022). The number of network outputs $C = K$ is equal to the number of known classes, and the targets are computed as one-hot encoding:

$$\forall n, c \in \{1, \dots, C\} : t_{n,c} = \begin{cases} 1 & c = \tau_n \\ 0 & \text{otherwise} \end{cases} \quad (3)$$

where $1 \leq \tau_n \leq K$ is the class label of the sample n . Following standard procedure for training deep networks on ILSVRC that contains almost balanced training classes, we select the weights for each class to be identical: $\forall c : w_c = 1$.

The second approach is often found in object detection models (Dhamija et al., 2020) which collect a lot of negative samples from the background of the training images. Similarly, this approach is used in other methods for open-set learning, such as G-OpenMax (Ge et al., 2017).³ In this Garbage class approach, negative data is used to train an additional network output z_{K+1} , so that we have a total of $C = K + 1$ outputs. Since the number of negative samples is usually higher than for known classes, we use class weights to balance them:

$$\forall c \in \{1, \dots, C\} : w_c = \frac{N}{CN_c} \quad (4)$$

where N_c is the number of training samples for class c . Finally, we use one-hot encoded targets $t_{n,c}$ according to (3), including label $\tau_n = K + 1$ for negative samples.

Finally, we employ the Entropic Open-Set (EOS) loss (Dhamija et al., 2018), which is a simple extension of the SoftMax loss. Similar to our first approach, we have one output for each of the known classes: $C = K$. For known samples, we employ one-hot-encoded target values according to (3), whereas for negative samples we use identical target values:

$$\forall n, c \in \{1, \dots, C\} : t_{n,c} = \frac{1}{C} \quad (5)$$

Sticking to the implementation of Dhamija et al. (2018), we select the class weights to be $\forall c : w_c = 1$ for all classes including the negative class, and leave the optimization of these values for future research. For the negative samples required by Garbage and EOS, we solely rely on the negative classes defined in the evaluation protocols (cf. Section 4.1), but we acknowledge that different negative samples, such as generative approaches (Ge et al., 2017), counterfactual images (Neal et al., 2018), noisy samples (Wilson et al., 2023), manifold mix-up (Verma et al., 2019) or other new approaches to obtain negative samples might further improve the training of the networks.

3. While these methods try to sample better negatives for training, they rely on this additional class for unknown samples.

3.2 Post-processing Methods

Our first post-processing method is based on Hendrycks and Gimpel (2017), which we call Maximum SoftMax Score (MSS). It is also our baseline approach that relies on the scores or probabilities derived from (1). It basically acts on the output of the trained networks defined above and helps in the decision-making based on the probability for the class: $p_c = y_c$. The second approach following the idea from Hendrycks et al. (2022), which we coin as Maximum Logit Score (MLS), on the other hand, does not push the network outputs through SoftMax. Instead, it works with the logits directly and considers the logit values $p_c = z_c$. Please note that these logit scores are not direct probability values, but none of our evaluation metrics in Section 4.2 actually requires probabilities.

As a third method, we make use of the original OpenMax technique as introduced by Bendale and Boult (2016), using a slight twist as implemented the VAST software package.⁴ OpenMax makes use of deep features $\vec{\varphi}$ extracted from the penultimate layer of the deep network, *i. e.*, the layer before the last fully-connected layer as shown in Figure 2 with weight matrix \mathbf{W} turns the deep features into logits:

$$\vec{z} = \mathbf{W}\vec{\varphi} \tag{6}$$

In the original OpenMax paper, Bendale and Boult (2016) called the deep features Activation Vectors (AV). For each known class $1 \leq c \leq K$, the Mean Activation Vector (MAV) $\vec{\mu}_c$ is computed by averaging the deep features extracted from all correctly classified known training samples of class c . Additionally, the cosine distances of the MAV $\vec{\mu}_c$ to all the AVs $\vec{\varphi}_{n,c}$ of the same class are computed. Here, we make use of the twist implemented in the VAST package: instead of using the original distances to model the distribution, we multiply the cosine distances by a certain factor κ , which allows modeling more compact class representations:

$$d_{n,c} = \kappa(1 - \cos(\vec{\varphi}_n, \vec{\mu}_c)) \tag{7}$$

The λ largest distances per class are used to model a Weibull distribution Ψ_c . For a given test sample, these Weibull distributions are taken to estimate a logit z_{K+1} for being unknown, as well as modifying the other logits for the top α classes. For details on this procedure, please refer to the original paper (Bendale and Boult, 2016). This additional logit is included into the SoftMax calculation (1), to obtain the probabilities $p_c = y_c$ for all known classes $c \in \{1, \dots, K\}$ and the additional unknown class y_{K+1} .⁵

The fourth method that we employ is the Extreme Value Machine (EVM) as introduced by Rudd et al. (2017). Similar to OpenMax, EVM uses Weibull-calibrated scoring to compute a Probability of Sample Inclusion (PSI) for each class, without computing a specific probability for a sample to be unknown. Contrary to OpenMax, which learns the probability models on distances between samples from the same class, EVM estimates distances of samples between classes. For a given activation vector $\vec{\varphi}_{n,c}$ of class c , it computes the cosine distances to all samples $\vec{\varphi}_{n',c'}$ from all other classes $c' \neq c$, which is again modified

4. <https://github.com/Vastlab/vast>

5. Note that in our evaluation, we ignore the probability for the unknown class returned by OpenMax or PROSER*. It is important to understand that the logit z_{K+1} is not ignored, but lowers all known class probabilities y_1, \dots, y_K through SoftMax, which enforces probabilities including y_{K+1} to sum up to 1.

by a distance multiplier κ to allow tighter class bounds (Günther et al., 2017):

$$d_{n,n',c} = \kappa(1 - \cos(\vec{\varphi}_{n,c}, \vec{\varphi}_{n',c'})) \quad (8)$$

Obviously, this is an expensive operation in $\mathcal{O}(N^2)$, but the VAST package⁴ provides an optimized implementation on the GPU for this task. From all of these distances, the *smallest* values are used to train a probability of sample *exclusion* using Weibull fitting, which is turned into a probability of sample *inclusion* $\Psi_{n,c}$ by taking its inverse probability. These are estimated for each training sample. To reduce computational cost, Rudd et al. (2017) added the possibility of model reduction via a cover threshold ω , but we do not make use of this option to ensure highest possible performance. Finally, to compute the probability p_c of a test sample $\vec{\varphi}$ to belong to a certain class c , the maximum over all probabilities associated with this class is taken:

$$p_c(\vec{\varphi}) = \max_{n: \tau_n=c} \Psi_{n,c}(\vec{\varphi}) \quad (9)$$

For EVM and OpenMax, we rely on the original implementation provided by the authors.⁴

The final method that we evaluate is PlaceholderRs for Open-SEt Recognition (PROSER) introduced by Zhou et al. (2021). It makes use of mid-level features $\vec{\varphi}$ from pretrained networks to fine-tune the network. Similar to OpenMax and the Garbage class approach, PROSER tries to estimate an additional logit z_{K+1} into SoftMax (1). To train this logit, PROSER does not rely on external negative samples, but it defines negative samples (which the authors call *data placeholders*) by merging mid-level features of the pretrained network extracted from two randomly selected features of different classes, based on the concept of manifold mix-up (Verma et al., 2019):

$$\vec{\varphi}' = \beta \vec{\varphi}_{n,c} + (1 - \beta) \vec{\varphi}_{n',c'} \quad \text{with } c \neq c' \quad (10)$$

where $0 \leq \beta \leq 1$ is randomly drawn from a Beta distribution. Additionally, instead of requiring all deep feature representations of unknown samples to gather in the same location in feature space, B logit values (that the authors call *classifier placeholders*) are computed for each negative/unknown sample, and the maximum of the B logits is taken to represent the garbage class:

$$z_{K+1} = \max_{1 \leq b \leq B} \vec{w}_b^T \vec{\varphi} \quad (11)$$

with \vec{w}_b being learnable parameters. As before, these logits are used to compute SoftMax activation y_c via (1), and we directly make use of them for evaluation $p_c = y_c$.⁵ Furthermore, for the known samples a specific loss function is applied encouraging one of the B classifier placeholders to be the second-highest logit (Zhou et al., 2021). Finally, the whole network is fine-tuned using the original training images from the known classes, and the generated mid-level features as negatives. Our implementation is inspired by the original code from the authors.⁶ However, the original implementation is not flexible enough to change the backbone network, so we needed to rewrite it to adapt it to other network topologies. We also corrected some mistakes made in the original code basis, for example, we now actually check that the two samples for the mix-up are not coming from the same class. Our own re-implementation can be found in our source code package.² To indicate these differences to the original code, we mark our reimplementation as PROSER*.

6. <https://github.com/zhoudw-zdw/CVPR21-Proser>

4. Data Set and Evaluation Protocols

4.1 Evaluation Protocols

In our evaluation, we use the ILSVRC 2012 data set (Russakovsky et al., 2015), for which we have developed three different open-set evaluation protocols (Palechor et al., 2023) as indicated in Figure 1. The three evaluation protocols differ in terms of difficulty in both closed and open-set classification. Additionally, negative classes are sampled such that they are similar to the known classes, since unrelated negative classes have been shown to not help in open-set classification (Dhamija et al., 2018). The samples in each protocol are split into training, validation and test splits, where known and negative classes are provided for training, validation and test, while unknown classes only appear during test time. For more details on the exact composition of the three protocols, please refer to Palechor et al. (2023).

Protocol P_1 is designed to be relatively difficult in closed-set classification as the task is to differentiate between all different types of dogs provided in ILSVRC. On the other hand, it should be relatively easy for open-set classification because unknown test samples in P_1 come from semantically distant categories such as devices, vehicles and food. Negative samples include classes similar to dogs, which basically are other four-legged animals.

Protocol P_3 is the exact opposite, it is more easy in closed-set classification since the enclosed known classes are more dissimilar to each other. At the same time, the unknown classes are semantically similar to the known classes, so it is likely that texture features are shared between known and unknown classes. Negative samples belong to the same group of categories as known and unknown classes.

Protocol P_2 is designed to be in the middle between P_1 and P_3 , as well as to be quite small so that hyperparameter optimization experiments can be conducted on this protocol. Known and negative classes are samples from the dog classes, while unknown classes include all other four-legged animals contained in ILSVRC 2012.

4.2 Evaluation Metric

To evaluate the different approaches, we make use of the Open-Set Classification Rate (OSCR) curve, which handles known and negative/unknown samples separately. Based on a certain threshold θ and assuming K different known classes, the Correct Classification Rate (CCR) and the False Positive Rate (FPR) are computed as (Palechor et al., 2023):

$$\text{CCR}(\theta) = \frac{|\{n \mid \tau_n \leq K \wedge \arg \max_{1 \leq c \leq K} p_{n,c} = \tau_n \wedge p_{n,\tau_n} \geq \theta\}|}{|N_K|} \quad (12)$$

$$\text{FPR}(\theta) = \frac{|\{n \mid \tau_n > K \wedge \max_{1 \leq c \leq K} p_{n,c} \geq \theta\}|}{|N_U|} \quad (13)$$

where n iterates all test samples and N_K and N_U are the total numbers of known and negative/unknown test samples, while a target label $\tau_n \leq K$ indicates a known sample and $\tau_n > K$ refers to a negative or unknown test sample.

By varying the threshold from the smallest to the highest possible score value, a curve can be drawn, plotting the CCR over the FPR. Since most applications require very low numbers of false positives, this curve is typically drawn with a logarithmic FPR axis. For

some approaches, many probability scores $p_{n,c}$ reach the maximum value of 1 to any reasonable precision, in which case there is no threshold θ that would allow computing low FPR values, so that the OSCR curve does not extend further to the left. This fact also disallows us computing the Area Under the OSCR curve (nevertheless Vaze et al. (2022); Chen et al. (2022) seem to do exactly that) since the extent of the FPR axis differs between algorithms. Additionally, in real-world applications a specific threshold θ is required, which is typically selected based on a certain FPR, but computing AUOSCR disables selecting such a threshold.

4.3 Single-Valued Evaluation Metric

Some of our open-set algorithms, such as OpenMax, EVM and PROSER*, rely on an already optimized network, but they require an additional hyperparameter optimization step onwards. Particularly, different combinations of algorithm-specific hyperparameters are tried to reach the best prediction performance. However, defining the best can only be achieved through a single value calculation which can make the comparison across algorithms and different hyperparameter settings possible.

For a fair comparison of various hyperparameter combinations, whose OSCR curves often end at different points on the FPR axis, we use a set of predefined FPR values to extract available CCR values that correspond to those points. Particularly, we computed CCR different values for FPR $\zeta \in \{10^{-3}, 10^{-2}, 10^{-1}, 10^0\}$. Since it is not always possible to find the exact FPR value, we make use of the infimum value if such value exists, and compute the sum over their corresponding CCR:

$$\text{CCR@FPR} = \sum_{\zeta} \begin{cases} \text{CCR}(\theta_{\text{FPR}=\zeta}) & \text{if } \theta_{\text{FPR}=\zeta} \text{ exists} \\ 0 & \text{otherwise} \end{cases} \quad (14)$$

$$\theta_{\text{FPR}=\zeta} = \arg \min_{\theta} \text{FPR}(\theta) \quad \text{s.t. } \text{FPR}(\theta) - \zeta \geq 0$$

In doing so, we only take into account existing FPRs and prevent our CCR@FPR measure from being affected by some artificial CCR values at non-reachable FPRs.

4.4 Comparison to Other Metrics

In many related publications, open-set systems are evaluated by computing the closed-set accuracy and the Area under the Receiver Operating Characteristics (AUROC) curve. The former only looks into the known classes, and is identical to the CCR at FPR=1. The latter concerns how well known and unknown classes can be distinguished by computing False Positive Rates according to (13), as well as the True Positive Rate (TPR):

$$\text{TPR}(\theta) = \frac{|\{n \mid \tau_n \leq K \wedge \max_{1 \leq c \leq K} p_{n,c} \geq \theta\}|}{|N_K|} \quad (15)$$

The ROC is computed by varying θ , and the area under that curve is determined. While we **vigorously discourage** the usage of this metric since it does not evaluate open-set performance (AUROC only evaluates out-of-distribution detection), we include it in our evaluation, solely to show that the usage of that metric **can lead to wrong conclusions**, cf. Section 6.2.

5. Experiments

Having both training-based and post-processing methods, we set up a comprehensive experimental design where not only training-based methods are evaluated, but also post-processing methods make use of results generated by training-based methods. Hence, we perform a total of 15 experiments on each of the three evaluation protocols, which include a cross-combination of three training-based methods: SoftMax, Garbage, and EOS, and five post-processing methods: MSS, MLS, OpenMax, EVM and PROSER*.

5.1 Network Training

We start our experiments by first training ResNet-50 models for each training-based method on all three protocols under the same conditions, *i. e.* we use same set of parameter values for the optimizer (Adam), number of epochs (120), and learning rate (10^{-3}).

When training a deep network, typically one chooses the network after that training epoch that produces the best performance according to a certain validation metric. Unfortunately, there exists no validation metric that would work in all circumstances. While in our previous publication (Palechor et al., 2023) we proposed a validation metric that looks into confidence values produced by the network for known and negative validation set samples, we have also shown that this metric does not perform well for all different loss functions. For example, training a network with the SoftMax approach, *i. e.*, excluding negative samples, will produce the best validation score after a few epochs, but this does not correspond to the best network that can be obtained (Palechor et al., 2023). Selecting different validation metrics, however, would have decreased the comparability across methods. Therefore, we have decided against relying on a validation metric and always make use of the network after 120 training epochs.

In our software package,² we compute and report several validation metrics, including the above-mentioned metric, which we observed would be well-suited for approaches that train with real negative samples. On the other hand, we never experienced any large amount of overfitting to the training data on any type of validation metric reported by our software package. In future work, we will try to investigate more on reasonable validation metrics that can be applied across different training regimes.

5.2 Hyperparameter Optimization

On top of the three trained networks we incorporate post-processing methods, OpenMax, EVM, and PROSER*. These methods require hyperparameter optimization, which we perform on the validation sets of all protocols separately to ensure optimal settings.

For OpenMax, we conduct grid search optimization for the required set of hyperparameters, including tail size λ , distance multiplier κ , and α as suggested by Bendale and Boulton (2016), while relying on the cosine-based distance metric (7). Below are the set of values that were used to trained OpenMax models which are then validated on the validation set:

- Tail Size: [10, 100, 250, 500, 750, 1000]
- Distance Multiplier = [1.5, 1.7, 2.0, 2.3]
- Alpha = [2, 3, 5, 10]

Protocol	Training	λ	κ	α	Σ
P_1	Softmax	1000	2.0	10	1.5823
	Garbage	1000	1.5	5	1.6087
	EOS	500	2.0	10	2.2867
P_2	Softmax	1000	2.3	10	1.1703
	Garbage	750	1.7	5	1.2638
	EOS	500	2.0	3	1.6239
P_3	Softmax	750	2.3	5	1.2201
	Garbage	1000	2.3	2	1.5077
	EOS	250	2.0	10	1.9241

(a) OpenMax

Protocol	Training	λ	κ	ω	Σ
P_1	Softmax	1000	0.4	1	1.5068
	Garbage	75	0.7	1	1.3909
	EOS	1000	0.2	1	1.4321
P_2	Softmax	300	0.3	1	1.1642
	Garbage	1000	0.2	1	1.2164
	EOS	150	0.2	1	1.1182
P_3	Softmax	100	0.5	1	1.3113
	Garbage	500	0.5	1	1.4061
	EOS	1000	0.2	1	1.3228

(b) EVM

Protocol	Training	B	Σ
P_1	Softmax	100	1.1342
	Garbage	2	1.1445
	EOS	5	2.3405
P_2	Softmax	1	1.2310
	Garbage	5	1.4862
	EOS	10	1.6420
P_3	Softmax	10	1.3456
	Garbage	10	1.7394
	EOS	100	1.7226

(c) PROSER*

Table 1: HYPERPARAMETER OPTIMIZATION. This table lists the hyperparameters of OpenMax, EVM and PROSER* applied to networks trained with three loss functions, optimized on the known and negative samples of the validation set.

EVM (Rudd et al., 2017) has similar hyperparameters to OpenMax, which include a tail size λ and the distance multiplier κ . We ended up with the following hyperparameter space to train multiple EVM models:

- Tail Size = [10, 25, 50, 75, 100, 150, 200, 300, 500, 1000]
- Distance Multiplier = [0.10, 0.20, 0.30, 0.40, 0.50, 0.70, 0.90, 1.00]

Due to extensive training time, for PROSER* we use the default values for β , α , λ from the original implementation. A more tedious hyperparameter optimization is left to the reader. The only hyperparameter which we vary in our case is the number of dummy classifiers (B). Since (Zhou et al., 2021) only trained on smaller datasets, we adapted the counts to our protocols and included:

- Dummy Classifiers = [1, 2, 5, 10, 25, 100]

By using CCR@FPR criterion from (14) for all hyperparameter combinations derived from the above list, we found the best performing hyperparameter values for both OpenMax, EVM, and PROSER in conjunction with three loss functions. In Table 1, we present

our findings for all three protocols, while the detailed results for the hyperparameter optimization can be found in the appendix. For most of the hyperparameters, there seems to be no clear trend on optimality per protocol or training loss, which indicates that tuning is required for every new dataset, protocol or practical application. The distance multipliers κ follow opposed trends for OpenMax and EVM, since for OpenMax, original distances are computed between training samples from the same class and need to be raised, while for EVM distances between different class’ training samples need to be reduced, in order to fit to the validation and test data distributions.

6. Results and Observations

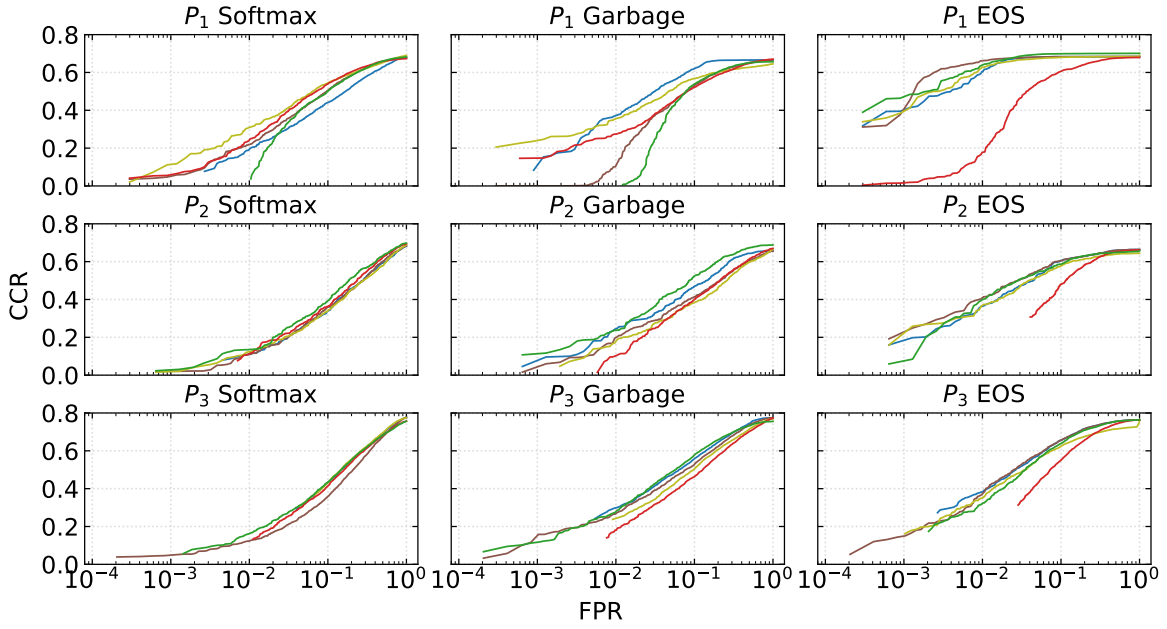
Utilizing the optimized hyperparameters of the post-processing methods, we switch our evaluation to the test set. Figure 3 shows OSCR curves with logarithmic scale for FPR axes for the 15 experimental settings on three protocols. Figure 3(a) here illustrates the test set performance for the negative, and Figure 3(b) for the unknown test samples. Each of them is split into the three protocols and the three training-based methods, while different colors indicate different post-processing methods. A more compact but also much more busy plot is provided in the appendix. Additionally, we list AUROC scores as well as CCR values for selected FPR values in Table 2, for both negative and unknown test samples. Within each protocol, we observe that majority of the classifiers show similar CCR performances in the closed-set case where FPR=1.

Since we provide many results in Figure 3 and Table 2, we cannot discuss every single combination of methods separately. This section provides some highlights on the main conclusions that can be drawn from our experiments.

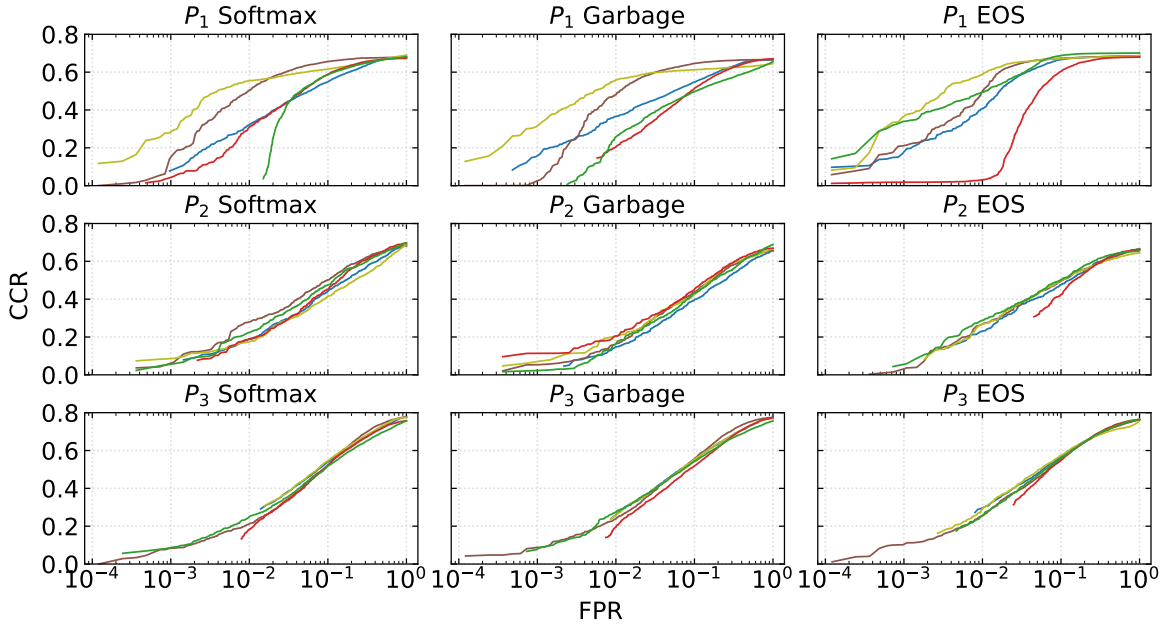
6.1 Negative vs. Unknown Test Samples

In our experiments, we evaluated our results with both negative and unknown test samples to compute CCR and FPR values – as given in Table 2 – and OSCR plots provided in Figure 3. For all protocols, we had selected the negative samples to be semantically closer to the known samples than the unknowns, cf. Figure 1, except for protocol P_3 where knowns, negatives and unknowns are semantically similar. Consequently, when ignoring the negatives during training as done with the SoftMax approach (left column in Figure 3), results on the unknown set are actually higher than on the negative set. Also for PROSER* (green lines in Figure 3), which samples negatives from mixing known samples instead, a similar behavior can be observed.

Observations change completely when using algorithms that make use of our provided negative samples during training. Please remember that the negative *sample instances* used during training and validation differ from the ones used for testing – only the classes are shared. Particularly, training with Entropic Open-Set loss (right column in Figure 3) improves extremely on the evaluation of negative test samples, but also the Garbage class approach (middle column in Figure 3) can benefit. Hence, when we know which kinds of uninteresting samples will most likely be seen during testing, these types of samples shall be used as negatives in combination with EOS to train the network. However, when we cannot know which kinds of unknown samples to expect, different solutions need to be found, for example, using manifold mix-up (Verma et al., 2019) or adversarial samples



(a) Negatives



(b) Unknowns

Figure 3: OSCR PLOTS. This figure shows OSCR plots for negative and unknown test samples on all three protocols, split across training-based methods. Colors separate post-processing methods.

Post-pr.	Training	Negative				Unknown				Acc
		AUROC	10^{-3}	10^{-2}	10^{-1}	AUROC	10^{-3}	10^{-2}	10^{-1}	1
MSS	Softmax	0.7811		0.1905	0.4409	0.8806	0.0772	0.3193	0.5495	0.6784
	Garbage	<u>0.9566</u>	0.0831	<u>0.3710</u>	<u>0.6193</u>	0.8883	0.1533	0.3652	0.5471	0.6662
	EOS	<i>0.9927</i>	<i>0.3948</i>	<i>0.6047</i>	<i>0.6836</i>	<i>0.9656</i>	<i>0.1703</i>	<i>0.4076</i>	<i>0.6666</i>	<i>0.6840</i>
MLS	Softmax	0.8596	0.0471	0.2186	0.5047	<u>0.9693</u>	0.1422	<i>0.5031</i>	<u>0.6564</u>	0.6784
	Garbage	0.8768	0.0000	0.1014	0.5300	<u>0.9676</u>	0.0231	0.4803	<u>0.6459</u>	0.6662
	EOS	0.9962	<i>0.3766</i>	0.6616	<i>0.6834</i>	0.9792	<i>0.2105</i>	0.4962	<i>0.6733</i>	<i>0.6840</i>
OpenMax	Softmax	0.8658	<u>0.1114</u>	<u>0.3091</u>	<u>0.5434</u>	0.9201	<u>0.2791</u>	<u>0.5538</u>	0.6160	<i>0.6898</i>
	Garbage	0.8743	<u>0.2364</u>	0.3543	0.5686	0.9146	0.3107	<u>0.5553</u>	0.6128	0.6450
	EOS	<i>0.9638</i>	<i>0.3845</i>	<i>0.6267</i>	<i>0.6795</i>	<i>0.9544</i>	0.3624	0.5864	<i>0.6716</i>	0.6891
EVM	Softmax	<u>0.8774</u>	0.0555	0.2381	0.5391	0.9161	<i>0.0412</i>	<i>0.3067</i>	0.5890	0.6729
	Garbage	0.8608	<i>0.1462</i>	<i>0.2740</i>	0.5210	0.8652		0.2038	0.5131	<u>0.6703</u>
	EOS	<i>0.9182</i>	0.0150	0.1755	<i>0.6053</i>	<i>0.9188</i>	0.0183	0.0314	<i>0.6041</i>	<i>0.6793</i>
PROSER*	Softmax	0.8442			0.5016	0.8795			0.5853	0.6817
	Garbage	0.8879			0.5383	0.8005		0.2571	0.4967	0.6567
	EOS	<i>0.9754</i>	0.4638	<i>0.6384</i>	0.6990	<i>0.9585</i>	<i>0.3390</i>	<i>0.4926</i>	0.6872	0.7012

(a) Protocol 1

Post-pr.	Training	Negative				Unknown				Acc
		AUROC	10^{-3}	10^{-2}	10^{-1}	AUROC	10^{-3}	10^{-2}	10^{-1}	1
MSS	Softmax	0.7024		0.1100	0.3387	0.7726		0.1887	0.4400	<i>0.6827</i>
	Garbage	0.8645	0.0460	<u>0.2427</u>	0.4680	0.7624		0.1467	0.3967	0.6560
	EOS	<i>0.9181</i>	<i>0.1600</i>	<i>0.3640</i>	0.6060	<i>0.8180</i>		<i>0.2307</i>	<i>0.4760</i>	<u>0.6640</u>
MLS	Softmax	0.7315	0.0200	0.1087	0.3593	0.8517	0.0427	<i>0.2800</i>	<i>0.5013</i>	<i>0.6827</i>
	Garbage	0.7828	0.0160	0.1960	0.4133	0.8210	<i>0.0527</i>	0.1613	0.4367	0.6560
	EOS	0.9244	0.1920	0.4040	<i>0.6040</i>	0.8292	0.0147	0.2660	0.4967	<u>0.6640</u>
OpenMax	Softmax	0.7301	0.0160	0.1233	0.3373	0.7589	<i>0.0827</i>	0.1733	0.4160	<i>0.6880</i>
	Garbage	0.7321		0.1700	0.3827	0.7976	0.0613	<u>0.2047</u>	0.4253	0.6673
	EOS	<i>0.9119</i>	<i>0.1593</i>	<i>0.3647</i>	<i>0.5753</i>	<i>0.8268</i>		<i>0.2647</i>	<i>0.5013</i>	0.6440
EVM	Softmax	0.7461		<i>0.1093</i>	0.3627	0.8199		0.1893	<i>0.4520</i>	<i>0.6940</i>
	Garbage	0.7732		0.1007	0.4000	<i>0.8282</i>	0.1133	<i>0.2033</i>	<u>0.4493</u>	0.6693
	EOS	<i>0.8363</i>			<i>0.4807</i>	0.7920			0.4233	0.6620
PROSER*	Softmax	<u>0.7577</u>	<u>0.0233</u>	0.1347	0.3913	0.7978	<i>0.0480</i>	0.2233	0.4740	0.6980
	Garbage	<u>0.8754</u>	<i>0.1073</i>	0.2373	<u>0.5233</u>	0.7699	0.0167	0.1600	0.4307	<u>0.6880</u>
	EOS	<i>0.8896</i>	0.0593	<i>0.3953</i>	<i>0.5867</i>	<i>0.8302</i>	<u>0.0440</u>	0.2873	0.5020	0.6573

(b) Protocol 2

Post-pr.	Training	Negative				Unknown				Acc
		AUROC	10^{-3}	10^{-2}	10^{-1}	AUROC	10^{-3}	10^{-2}	10^{-1}	1
MSS	Softmax	0.7361			0.4331	0.8008			0.5399	0.7768
	Garbage	0.8389		0.2963	0.5584	0.8101		0.2407	0.5493	<u>0.7751</u>
	EOS	<i>0.9116</i>		0.3826	<i>0.6558</i>	<i>0.8342</i>		0.2942	<i>0.5681</i>	0.7633
MLS	Softmax	0.7202	0.0458	0.1228	0.3587	<u>0.8360</u>	0.0837	0.2106	0.5191	0.7768
	Garbage	0.8231	<u>0.1158</u>	0.2661	0.5286	0.8487	<u>0.0877</u>	0.2380	<u>0.5558</u>	<u>0.7751</u>
	EOS	0.9146	0.1437	<i>0.3698</i>	0.6567	0.8341	0.1019	<i>0.2552</i>	<i>0.5575</i>	0.7633
OpenMax	Softmax	0.7400			0.4322	0.8104			<u>0.5460</u>	<i>0.7744</i>
	Garbage	0.7799		0.2375	0.5034	0.8130		0.2375	0.5532	0.7694
	EOS	<i>0.8292</i>		<i>0.3506</i>	<i>0.6236</i>	<i>0.8147</i>		<i>0.2914</i>	0.5738	0.7604
EVM	Softmax	0.7433			0.4150	0.8151		0.1819	0.5241	0.7567
	Garbage	0.7707		<i>0.1800</i>	0.4628	0.8166		<i>0.1951</i>	0.5193	<i>0.7731</i>
	EOS	<i>0.8375</i>			<i>0.5498</i>	<i>0.8276</i>			<i>0.5482</i>	0.7636
PROSER*	Softmax	<u>0.7569</u>		<u>0.1612</u>	<u>0.4336</u>	0.7945	<i>0.0861</i>	<u>0.2462</u>	0.5180	0.7562
	Garbage	<u>0.8456</u>	<i>0.1123</i>	0.2766	<u>0.5784</u>	0.7971	0.0766	<i>0.2728</i>	0.5416	0.7560
	EOS	<i>0.8921</i>		<i>0.3209</i>	<i>0.6395</i>	<i>0.8304</i>		0.2546	<i>0.5575</i>	<i>0.7649</i>

(c) Protocol 3

Table 2: DETAILED RESULTS. This table shows detailed AUROC and CCR values on Negative and Unknown test samples for several FPR thresholds ζ , as well as the closed-set accuracy. In each column, the best values are highlighted in **blue**, the best per post-processing method in *italics*, and the best per training loss are underlined. When low FPR values cannot be reached with any threshold, fields are left empty.

(Chen et al., 2022) as negatives. In this case, additional open-set post-processing methods on top of these deep features, for example OpenMax (tan lines in Figure 3), might be used to improve performance.

6.2 OSCR vs. AUROC

For comparison, we also added AUROC values to Table 2. We can observe that all maximal AUROC values (highlighted in blue) appear in the MLS algorithm, combined with various training methods. This seems to validate the claim of Vaze et al. (2022) that MLS performs very well in any open-set task and that no other open-set algorithm is able to outperform MLS. However, when having a closer look into the CCR values at various FPR thresholds, especially when evaluating unknown test samples, it is apparent that such a conclusion is misleading. Good results can be observed for various combinations of training and post-processing algorithms, and depending on the selected FPR threshold and the difficulty of the evaluation protocol, conclusions can differ tremendously.

6.3 Easy vs. Hard Unknowns

One particular advantage of our proposed evaluation protocols is the possibility to evaluate open-set scenarios in different difficulties. Indeed, when looking into the results on the different protocols, we can see major differences in the advances of open-set evaluations. When unknown classes are very different from the known classes, as given in protocol P_1 , post-processing approaches such as OpenMax or MLS can bring large improvements over the standard thresholding of SoftMax scores (MSS). Particularly, the combination of training the network with EOS and using OpenMax on top of these deep features seems to be the most fruitful approach here.

This changes drastically when evaluating the more difficult open-set protocol P_3 , where MLS actually decreases performance with respect to the simple MSS approach. Also, OpenMax cannot really improve over the MSS baseline. Only the EOS loss seems to provide slight improvements over the Garbage class approach, which in turn has shows tiny improvements over the SoftMax baseline. However, especially when testing with unknown samples, all results are very similar and no clear winner can be identified.

6.4 Garbage Class vs. Entropic Open-Set Loss

In virtually none of our evaluations, the prevailing approach in the literature – collecting all negative samples in a separate Garbage class during training – has been the best approach. Throughout, the Garbage approach was inferior to EOS. Forcing all negative (and unknown) samples to reside in a separate part of the feature space, as done by Garbage (cf. for example Dhamija et al. (2018)), does not seem to be the best idea. Instead, encouraging the deep features of negative (and unknown) samples to have small magnitudes enforces the natural behavior of deep networks, and is proven by Dhamija et al. (2018) to be an optimal way of restricting confidence scores of negative samples.

However, there were some differences in the training procedure. For example, the Garbage approach used class-balancing weights as given in (4), which reduced the influence of negative samples on the loss – if such class weights were not present, only the

majority class (the negative class in our case) would have been learned well (Rudd et al., 2016). On the other hand, for EOS training, we kept the weights of each negative sample as high as for the known samples, which made the training focus more on negative samples. Especially in protocols P_2 and P_3 , where known and negative samples are extremely similar, this lead to a noticeable decrease in closed-set performance. In future work, we will investigate whether a class weighting scheme between the two extremes can help in keeping high closed-set accuracy while still improving open-set capabilities.

6.5 EVM and OpenMax

Both EVM and OpenMax estimate Weibull distributions on deep feature representations for estimating the probability of sample inclusion. Only the data used to estimate these distributions differ. While OpenMax only looks into the distribution of deep feature distances inside classes, EVM models such distances between classes. Hence, EVM requires the distribution of different-class known samples to appropriately predict the distribution of unknown samples, which might be too difficult in general. EVM hyperparameters optimized on the negative samples of the validation data are likely to translate badly to unknown samples from test data. Since the distribution of negative and unknown classes purposefully differs, especially in protocol P_1 , EVM (red lines in Figure 3) is highly inferior to MSS (blue lines in Figure 3). However, even when negative and unknown data is similar as in P_3 , EVM is not able to show improvements.

On the other hand, OpenMax depends only on same-class feature comparisons, which makes it independent of the distribution of different-class and unknown samples. Therefore, it can handle well unknown samples that are far away from the knowns, as in protocol P_1 . However, it loses its advantage in more complex situations where known and unknown data are more semantically similar.

Note that we had to make use of the distance multiplier κ in (7) to model samples correctly. We assume that this problem arises since we model activation vectors from the same data that the network is trained with, which might not follow the distribution of the test data. In future work, we will investigate whether using validation data for training OpenMax and EVM will improve the similarity between model training and test data. Also, theoretically we could add the negative data to our EVM as additional other-class samples, which might improve its stability, at least when evaluated on negative data.

6.6 PROSER*

For protocols P_1 and P_2 , PROSER* provides the best performances at large FPR thresholds 0.1 and 1, and reasonable CCR scores at smaller FPR thresholds. Especially when the network is originally trained with EOS loss, PROSER* achieves the best results in our evaluation. Presumably, EOS, which makes use of real negative samples during training, shapes the feature space such that negative samples cluster in the center of the feature space. This provides a good initialization for PROSER*, which utilizes mix-up negative samples, which further shape the space for unknown samples.

In any case, these results do not transfer to more difficult cases, as provided in protocol P_3 , where PROSER* fine-tuning is actually decremental and results are generally reduced w.r.t. the MSS or MLS baseline.

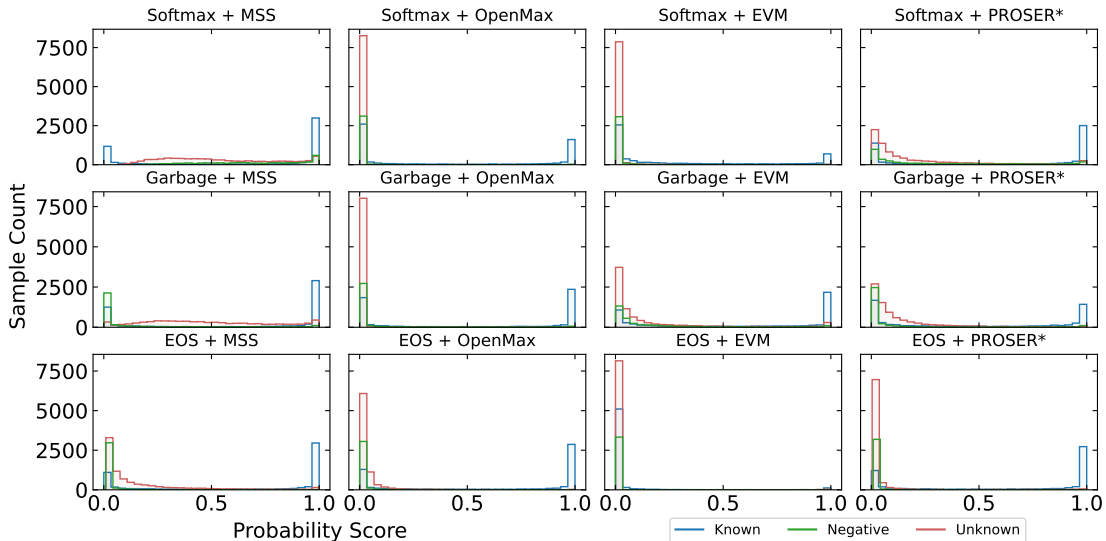


Figure 4: SCORE DISTRIBUTIONS. This figure shows score distributions extracted from the network trained with three different loss functions, and further post-processed with all algorithms (except for MLS), on protocol P_1 .

7. Combining Training-based with Post-processing Methods

In this paper, for the first time in research, two different basic approaches to open-set classification are combined, which are training-based methods such as EOS, and post-processing methods such as OpenMax or PROSER*. In order to show the advantages of this combination, we plot the distributions of the probability scores extracted from different networks obtained through different algorithms. Here we exclude MLS since it does not provide probability distributions, but only logit scores. Particularly, for known samples, we use the probability assigned to the correct class, while for negative and unknown samples, we select the maximal probability obtained over all known classes. The score distributions for protocol P_1 can be found in Figure 4, while for the other two protocols they are in the appendix. The discussion here mainly targets protocol P_1 in Figure 4, but similar conclusions can be drawn from the other two protocols. Interestingly, we can observe an almost binary score distribution, where probabilities are either close to 0 or close to 1. This validates the well-known fact Matan et al. (1990) that SoftMax scores are poor probability estimates.

When training a network with the SoftMax approach, the network learns to provide large confidence scores for known samples, but also assigns larger scores to negative and unknown samples. When trying to dissect these using OpenMax, EVM, or PROSER*, most of the negative and unknown samples get very low maximal scores, but also many of the known samples reduce their confidences, usually drastically. Training the network with a Garbage class does not improve score distributions when thresholding probabilities, but OpenMax and EVM can keep high probability scores for known samples – yet a few unknown samples still obtain a probability close to 1 of being classified as a known class. Finally, EOS provides a feature space where most negative and unknown samples have low

confidence scores, and OpenMax and PROSER* can further reduce the number of unknown samples that have high scores while not reducing scores for known classes – EVM on the other hand seems not to profit from better separation in the original feature space.

8. Conclusion

The aim of this paper is to provide the first large-scale and reproducible evaluation of different open-set classification techniques. Based on the ILSVRC 2012 data set and the WordNet hierarchy, we developed three open-set evaluation protocols that contain different difficulties in terms of closed-set and open-set classification. We experimented with three different loss functions to train initial networks to obtain deep features that are suited for open-set classification. On top of these networks, we applied five different post-processing techniques. We showed that both better features and additional open-set techniques can improve open-set performance. For the first time in the literature, we also combined feature learning and post-processing techniques. In the cases that we know which kinds of unknown samples can be expected, and when known and unknown classes are semantically very different, the combination of Entropic Open-Set loss to obtain separable features and post-processing with OpenMax or PROSER* to reject unknown samples provided the best improvements. On the other hand, when known and unknown classes are semantically similar, none of the evaluated techniques provided reasonable improvements over thresholding standard SoftMax confidence scores (MSS).

In this evaluation we only made use of a single network topology – ResNet-50 with an additional embedding layer. Future research should investigate whether other network topologies follow the same trends. Also, other open-set classification techniques have been proposed in the literature, which need to be tested in large scale as well. For example, in our protocols we solely made use of real negative samples – except during PROSER* post-processing – while the literature is largely focused on how to artificially create such negative samples. Including different negative sample generation techniques will open a third type of algorithm, which can be combined with the currently implemented two types. Since we provide our complete source code – from raw images to network training, open-set modeling and the final plots and tables in this paper and its appendix – testing your own algorithm in a realistic, comparable and reproducible manner is just one step away!

References

- Abhijit Bendale and Terrance E. Boult. Towards open set deep networks. In *Conference on Computer Vision and Pattern Recognition (CVPR)*. IEEE, 2016.
- Terrance E. Boult, Steve Cruz, Akshay Raj Dhamija, Manuel Günther, James Henrydoss, and Walter J. Scheirer. Learning and the unknown: Surveying steps toward open world recognition. In *AAAI Conference on Artificial Intelligence*, volume 33, pages 9801–9807, 2019.
- Guangyao Chen, Limeng Qiao, Yemin Shi, Peixi Peng, Jia Li, Tiejun Huang, Shiliang Pu, and Yonghong Tian. Learning open set network with discriminative reciprocal points. In *European Conference on Computer Vision (ECCV)*. Springer, 2020.
- Guangyao Chen, Peixi Peng, Xiangqian Wang, and Yonghong Tian. Adversarial reciprocal points learning for open set recognition. *Transactions on Pattern Analysis and Machine Intelligence (TPAMI)*, 44(11), 2022.
- Jia Deng, Wei Dong, Richard Socher, Li-Jia Li, Kai Li, and Li Fei-Fei. ImageNet: A large-scale hierarchical image database. In *Conference on Computer Vision and Pattern Recognition (CVPR)*. IEEE, 2009.
- Akshay Raj Dhamija, Manuel Günther, and Terrance E. Boult. Reducing network agnostophobia. In *Advances in Neural Information Processing Systems (NeurIPS)*, pages 9157–9168, 2018.
- Akshay Raj Dhamija, Manuel Günther, and Terrance E. Boult. Improving deep network robustness to unknown inputs with Objectosphere. In *Conference on Computer Vision and Pattern Recognition Workshops (CVPRW)*, 2019.
- Akshay Raj Dhamija, Manuel Günther, Jonathan Ventura, and Terrance E. Boult. The overlooked elephant of object detection: Open set. In *Winter Conference on Applications of Computer Vision (WACV)*, pages 1021–1030, 2020.
- Zongyuan Ge, Sergey Demyanov, and Rahil Garnavi. Generative OpenMax for multi-class open set classification. In *British Machine Vision Conference (BMVC)*, 2017.
- Chuanxing Geng, Sheng-Jun Huang, and Songcan Chen. Recent advances in open set recognition: A survey. *Transactions on Pattern Analysis and Machine Intelligence (TPAMI)*, 43(10):3614–3631, 2021.
- Patrick Grother, Mei Ngan, and Kayee Hanaoka. Face recognition vendor test (FRVT) part 2: Identification. Technical report, National Institute of Standards and Technology, 2022.
- Manuel Günther, Steve Cruz, Ethan M. Rudd, and Terrance E. Boult. Toward open-set face recognition. In *Conference on Computer Vision and Pattern Recognition Workshops (CVPRW)*, pages 71–80, 2017.
- Manuel Günther, Akshay Raj Dhamija, and Terrance E. Boult. Watchlist adaptation: Protecting the innocent. In *International Conference of the Biometrics Special Interest Group (BIOSIG)*, 2020.

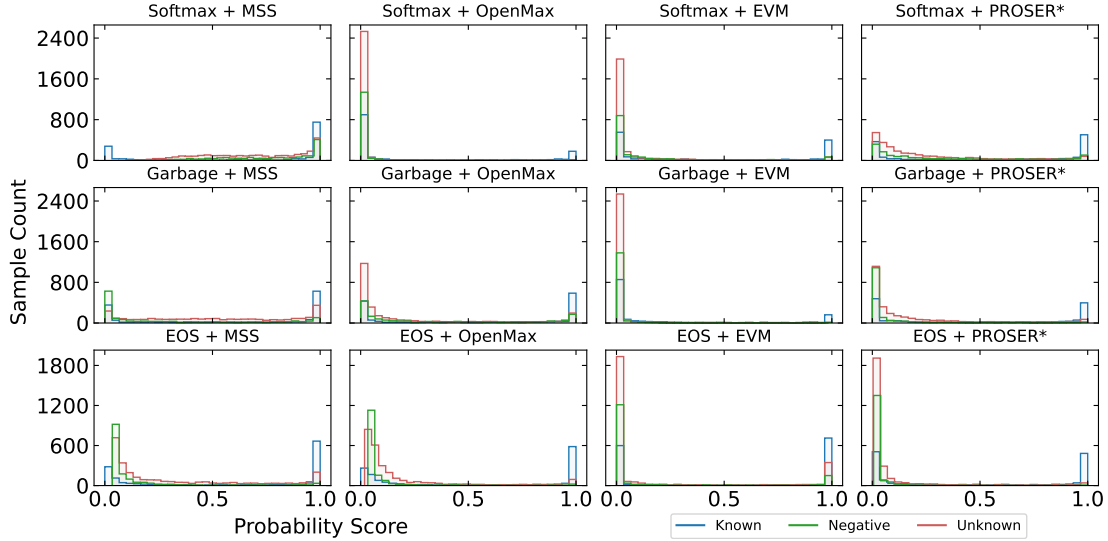
- Kaiming He, Xiangyu Zhang, Shaoqing Ren, and Jian Sun. Deep residual learning for image recognition. In *Conference on Computer Vision and Pattern Recognition (CVPR)*. IEEE, 2016.
- Dan Hendrycks and Kevin Gimpel. A baseline for detecting misclassified and out-of-distribution examples in neural networks. In *International Conference on Learning Representations (ICLR)*, 2017.
- Dan Hendrycks, Steven Basart, Mantas Mazeika, Andy Zou, Joseph Kwon, Mohammadreza Mostajabi, Jacob Steinhardt, and Dawn Song. Scaling out-of-distribution detection for real-world settings. In *International Conference on Machine Learning (ICML)*. PMLR, 2022.
- Gao Huang, Zhuang Liu, Laurens van der Maaten, and Kilian Q. Weinberger. Densely connected convolutional networks. In *Conference on Computer Vision and Pattern Recognition (CVPR)*, 2017.
- Huaizu Jiang and Erik Learned-Miller. Face detection with the Faster R-CNN. In *International Conference on Automatic Face & Gesture Recognition (FG)*, 2017.
- Alex Krizhevsky and Geoffrey Hinton. Learning multiple layers of features from tiny images. Technical report, University of Toronto, 2009.
- Alex Krizhevsky, Ilya Sutskever, and Geoffrey E. Hinton. ImageNet classification with deep convolutional neural networks. In *Advances in Neural Information Processing Systems (NIPS)*, 2012.
- Ya Le and Xuan Yang. Tiny imagenet visual recognition challenge. Technical report, Stanford, 2015.
- Yann LeCun, LD Jackel, Léon Bottou, Corinna Cortes, John S Denker, Harris Drucker, Isabelle Guyon, UA Muller, E Sackinger, Patrice Simard, et al. Learning algorithms for classification: A comparison on handwritten digit recognition. *Neural networks: the statistical mechanics perspective*, 261:276, 1995.
- Yann LeCun, Corinna Cortes, and Christopher J. C. Burges. The MNIST database of handwritten digits, 1998.
- Shiyu Liang, Yixuan Li, and Rayadurgam Srikant. Enhancing the reliability of out-of-distribution image detection in neural networks. In *International Conference on Learning Representations (ICLR)*, 2017.
- Ofer Matan, R.K. Kiang, C.E. Stenard, B. Boser, J.S. Denker, D. Henderson, R.E. Howard, W. Hubbard, L.D. Jackel, and Yann Le Cun. Handwritten character recognition using neural network architectures. In *USPS Advanced Technology Conference*, 1990.
- George A Miller. *WordNet: An electronic lexical database*. MIT press, 1998.
- Lawrence Neal, Matthew Olson, Xiaoli Fern, Weng-Keen Wong, and Fuxin Li. Open set learning with counterfactual images. In *European Conference on Computer Vision (ECCV)*, 2018.

- Yuval Netzer, Tao Wang, Adam Coates, Alessandro Bissacco, Bo Wu, and Andrew Y. Ng. Reading digits in natural images with unsupervised feature learning. In *Advances in Neural Information Processing Systems (NIPS) Workshop*, 2011.
- Andres Palechor, Annesha Bhoumik, and Manuel Günther. Large-scale open-set classification protocols for imagenet. In *Winter Conference on Applications of Computer Vision (WACV)*, pages 42–51. CVF/IEEE, January 2023.
- P. Jonathon Phillips, Patrick Grother, and Ross Micheals. *Handbook of Face Recognition*, chapter Evaluation Methods in Face Recognition. Springer, 2nd edition, 2011.
- Joseph Redmon, Santosh Divvala, Ross Girshick, and Ali Farhadi. You only look once: Unified, real-time object detection. In *Conference on Computer Vision and Pattern Recognition (CVPR)*. IEEE, 2016.
- Shaoqing Ren, Kaiming He, Ross Girshick, and Jian Sun. Faster R-CNN: Towards real-time object detection with region proposal networks. In *Advances in Neural Information Processing Systems (NIPS)*, 2015.
- Ethan M. Rudd, Manuel Günther, and Terrance E. Boulton. MOON: A mixed objective optimization network for the recognition of facial attributes. In *European Conference on Computer Vision (ECCV)*, pages 19–35. Springer, 2016.
- Ethan M. Rudd, Lalit P. Jain, Walter J. Scheirer, and Terrance E. Boulton. The extreme value machine. *Transactions on Pattern Analysis and Machine Intelligence (TPAMI)*, 2017.
- Olga Russakovsky, Jia Deng, Hao Su, Jonathan Krause, Sanjeev Satheesh, Sean Ma, Zhiheng Huang, Andrej Karpathy, Aditya Khosla, Michael Bernstein, et al. Imagenet large scale visual recognition challenge. *International Journal of Computer Vision (IJCV)*, 115(3), 2015.
- Sagar Vaze, Kai Han, Andrea Vedaldi, and Andrew Zissermann. Open-set recognition: A good closed-set classifier is all you need? In *International Conference on Learning Representations (ICLR)*, 2022.
- Vikas Verma, Alex Lamb, Christopher Beckham, Amir Najafi, Ioannis Mitliagkas, David Lopez-Paz, and Yoshua Bengio. Manifold mixup: Better representations by interpolating hidden states. In *International Conference on Machine Learning (ICML)*. PMLR, 2019.
- Zitai Wang, Qianqian Xu, Zhiyong Yang, Yuan He, Xiaochun Cao, and Qingming Huang. Openauc: Towards auc-oriented open-set recognition. In *Advances in Neural Information Processing Systems (NeuRIPS)*, 2022.
- Samuel Wilson, Tobias Fischer, Feras Dayoub, Dimitry Miller, and Niko Sünderhauf. SAFE: Sensitivity-aware features for out-of-distribution object detection. *arXiv preprint arXiv:2208.13930*, 2023.
- Han Xiao, Kashif Rasul, and Roland Vollgraf. Fashion-MNIST: A novel image dataset for benchmarking machine learning algorithms. *arXiv preprint arXiv:1708.07747*, 2017.

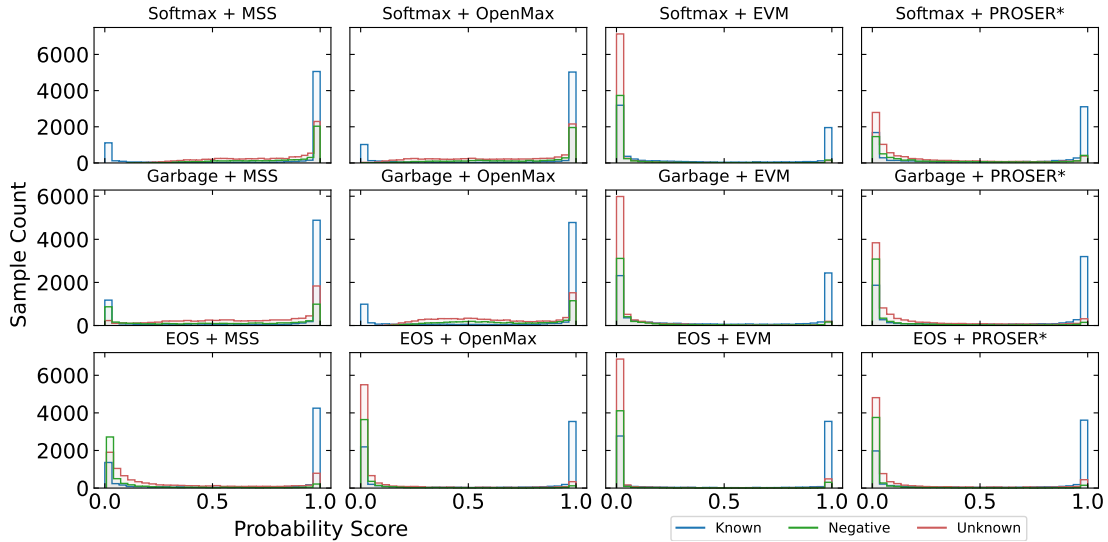
- Jingkang Yang, Pengyun Wang, Dejian Zou, Zitang Zhou, Kunyuan Ding, Wenxuan Peng, Haoqi Wang, Guangyao Chen, Bo Li, Yiyou Sun, Xuefeng Du, Kaiyang Zhou, Wayne Zhang, Dan Hendrycks, Yixuan Li, and Ziwei Liu. Openood: Benchmarking generalized out-of-distribution detection. In *Advances in Neural Information Processing Systems (NeurIPS)*, 2022.
- Li Yuan, Yunpeng Chen, Tao Wang, Weihao Yu, Yujun Shi, Zi-Hang Jiang, Francis E.H. Tay, Jiashi Feng, and Shuicheng Yan. Tokens-to-Token ViT: Training vision transformers from scratch on imagenet. In *International Conference on Computer Vision (ICCV)*, 2021.
- Zhong-Qiu Zhao, Peng Zheng, Shou-tao Xu, and Xindong Wu. Object detection with deep learning: A review. *Transactions on Neural Networks and Learning Systems (TNNLS)*, 30(11):3212–3232, 2019.
- Da-Wei Zhou, Han-Jia Ye, and De-Chuan Zhan. Learning placeholders for open-set recognition. In *Conference on Computer Vision and Pattern Recognition (CVPR)*, 2021.

Appendix

Here, we provide the additional score distributions plots for protocols P_2 and P_3 .



(a) Protocol P_2



(b) Protocol P_3

Figure 5: SCORE DISTRIBUTIONS. This figure shows score distributions extracted from the network trained with various loss functions on (a) Protocol P_2 and (b) protocol P_3 , and further processed with all algorithms (except for MLS).

We also include a plot that combines all results. While being busy, this plot improves the comparability across training functions.

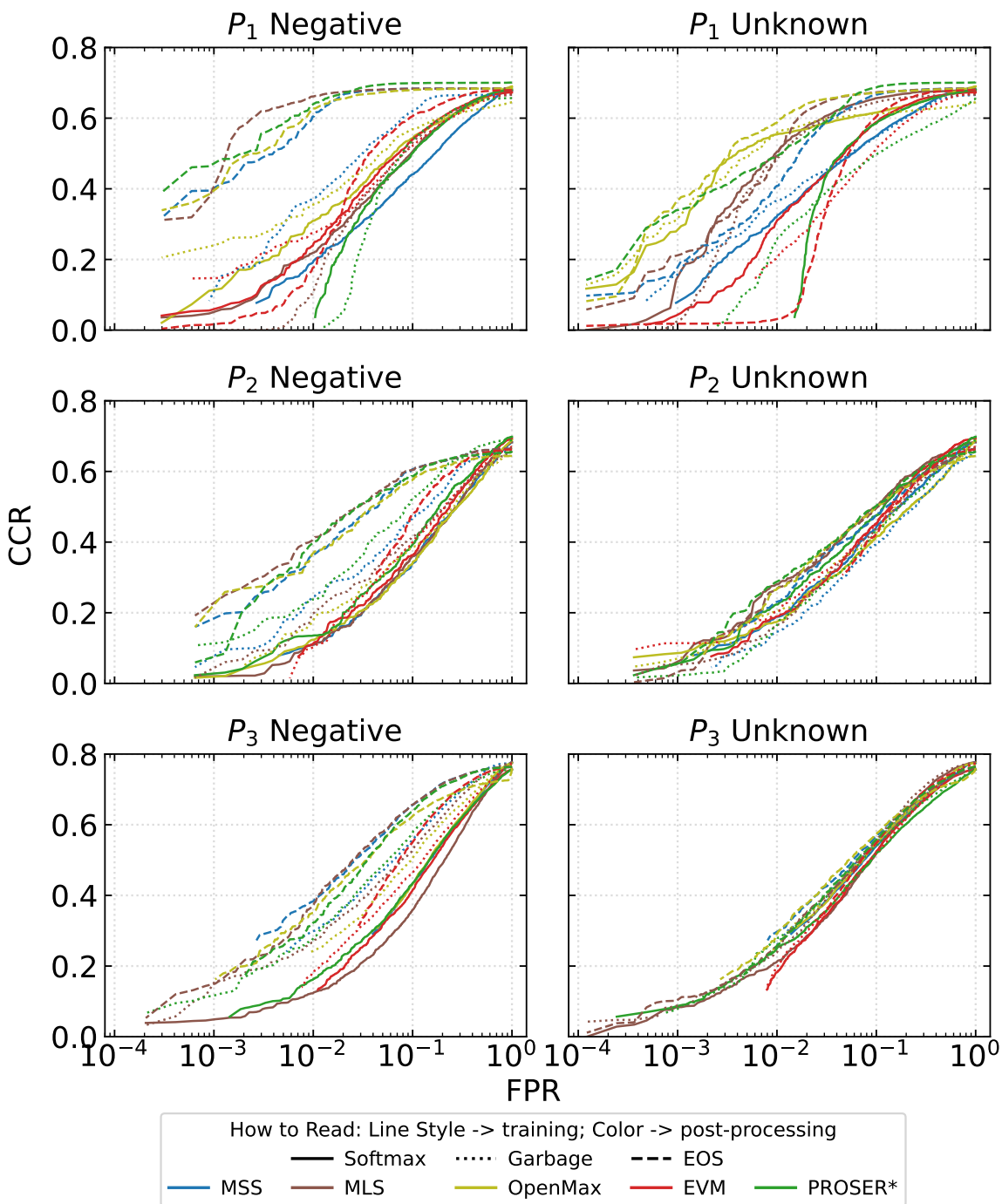


Figure 6: OSCR PLOTS. This figure shows OSCR plots for negative and unknown test samples on all protocols. Line styles distinguish training-based, colors post-processing methods.

Additionally, we provide all CCR scores at several FPR values for all parameters of OpenMax, EVM and PROSER*, as obtained on the validation set. The Σ column includes the sum of all existing CCR values at FPR values of $\zeta = \{10^{-3}, 10^{-2}, 10^{-1}, 1\}$, according to (14). Best values are highlighted in bold font.

λ	κ	ω	10^{-3}	10^{-2}	10^{-1}	1	Σ	10^{-3}	10^{-2}	10^{-1}	1	Σ	10^{-3}	10^{-2}	10^{-1}	1	Σ
25	0.2	1	0.0397	0.1740	0.3977	0.5267	1.1381	0.0046	0.0643	0.3509	0.4867	0.9065	0.0176	0.1276	0.5134	0.5662	1.2247
25	0.3	1	0.0606	0.1999	0.4361	0.5707	1.2673	0.0115	0.0855	0.3952	0.5308	1.0230	0.0245	0.1488	0.5371	0.6033	1.3138
25	0.4	1	0.0738	0.2227	0.4655	0.5972	1.3592	0.0300	0.1218	0.4378	0.5650	1.1547	0.0377	0.1750	0.4925	0.6227	1.3279
25	0.5	1	0.0850	0.2406	0.4918	0.6233	1.4407	0.0663	0.1673	0.4695	0.5951	1.2982		0.1586	0.3657	0.6410	1.1652
25	0.7	1		0.2601	0.5076	0.6512	1.4189		0.2580	0.4880	0.6322	1.3782				0.6584	0.6584
25	0.9	1			0.4867	0.6500	1.1367			0.4688	0.6358	1.1045				0.6601	0.6601
25	1.0	1				0.6271	0.6271				0.6140	0.6140				0.6420	0.6420
50	0.2	1	0.0401	0.2001	0.4443	0.5661	1.2505	0.0045	0.0515	0.4101	0.5348	1.0009	0.0177	0.1327	0.5447	0.5977	1.2927
50	0.3	1	0.0605	0.2101	0.4701	0.6053	1.3461	0.0115	0.0782	0.4430	0.5756	1.1083	0.0246	0.1575	0.5536	0.6286	1.3643
50	0.4	1	0.0745	0.2322	0.4863	0.6234	1.4165	0.0311	0.1171	0.4691	0.5995	1.2168		0.1797	0.4793	0.6414	1.3003
50	0.5	1	0.0838	0.2436	0.5013	0.6393	1.4679	0.0684	0.1605	0.4850	0.6176	1.3316		0.1590	0.3635	0.6519	1.1744
50	0.7	1		0.2615	0.5084	0.6565	1.4264		0.2602	0.4898	0.6369	1.3869				0.6627	0.6627
50	0.9	1			0.4880	0.6516	1.1396			0.4714	0.6375	1.1090				0.6625	0.6625
50	1.0	1				0.6338	0.6338				0.6204	0.6204				0.6469	0.6469
75	0.2	1	0.0412	0.2078	0.4655	0.5883	1.3029	0.0045	0.0515	0.4391	0.5596	1.0546	0.0182	0.1372	0.5559	0.6120	1.3232
75	0.3	1	0.0583	0.2192	0.4798	0.6173	1.3746	0.0116	0.0754	0.4619	0.5960	1.1449	0.0237	0.1628	0.5479	0.6385	1.3729
75	0.4	1	0.0747	0.2363	0.4960	0.6328	1.4397	0.0315	0.1167	0.4806	0.6120	1.2409		0.1804	0.4625	0.6475	1.2903
75	0.5	1	0.0828	0.2464	0.5052	0.6443	1.4787	0.0672	0.1619	0.4901	0.6257	1.3450		0.1598	0.3582	0.6559	1.1739
75	0.7	1		0.2618	0.5088	0.6565	1.4272		0.2614	0.4913	0.6382	1.3909				0.6633	0.6633
75	0.9	1			0.4872	0.6520	1.1392			0.4717	0.6384	1.1101				0.6624	0.6624
75	1.0	1				0.6352	0.6352				0.6218	0.6218				0.6491	0.6491
100	0.2	1	0.0430	0.2093	0.4739	0.6003	1.3264	0.0045	0.0531	0.4552	0.5754	1.0882	0.0184	0.1423	0.5626	0.6205	1.3439
100	0.3	1	0.0540	0.2232	0.4871	0.6266	1.3908	0.0116	0.0765	0.4741	0.6036	1.1658	0.0229	0.1670	0.5395	0.6434	1.3727
100	0.4	1	0.0747	0.2373	0.4996	0.6367	1.4483	0.0315	0.1170	0.4865	0.6185	1.2535		0.1836	0.4587	0.6519	1.2942
100	0.5	1	0.0828	0.2498	0.5075	0.6464	1.4865	0.0667	0.1624	0.4948	0.6298	1.3537		0.1605	0.3568	0.6579	1.1752
100	0.7	1		0.2611	0.5102	0.6567	1.4279		0.2600	0.4917	0.6391	1.3908				0.6643	0.6643
100	0.9	1			0.4867	0.6522	1.1389			0.4697	0.6385	1.1082				0.6631	0.6631
100	1.0	1				0.6367	0.6367				0.6228	0.6228				0.6502	0.6502
150	0.2	1	0.0407	0.2202	0.4844	0.6155	1.3608	0.0045	0.0517	0.4720	0.5917	1.1200	0.0186	0.1495	0.5696	0.6304	1.3680
150	0.3	1	0.0546	0.2272	0.4950	0.6327	1.4095	0.0114	0.0804	0.4852	0.6144	1.1914	0.0216	0.1718	0.5307	0.6475	1.3715
150	0.4	1	0.0746	0.2427	0.5045	0.6423	1.4641	0.0308	0.1190	0.4930	0.6261	1.2689		0.1846	0.4565	0.6540	1.2952
150	0.5	1	0.0821	0.2523	0.5110	0.6500	1.4954	0.0649	0.1631	0.4977	0.6335	1.3593		0.1621	0.3562	0.6599	1.1782
150	0.7	1		0.2595	0.5107	0.6568	1.4270		0.2537	0.4926	0.6405	1.3868				0.6651	0.6651
150	0.9	1			0.4844	0.6515	1.1359			0.4666	0.6384	1.1050				0.6625	0.6625
150	1.0	1				0.6369	0.6369				0.6235	0.6235				0.6510	0.6510
200	0.2	1	0.0396	0.2283	0.4894	0.6211	1.3784	0.0045	0.0557	0.4809	0.6012	1.1424	0.0188	0.1557	0.5722	0.6355	1.3821
200	0.3	1	0.0538	0.2331	0.4985	0.6373	1.4226	0.0113	0.0858	0.4901	0.6206	1.2077	0.0207	0.1799	0.5288	0.6496	1.3789
200	0.4	1	0.0746	0.2459	0.5085	0.6452	1.4743	0.0299	0.1220	0.4976	0.6291	1.2787		0.1848	0.4553	0.6558	1.2959
200	0.5	1	0.0809	0.2532	0.5136	0.6501	1.4978	0.0623	0.1632	0.4993	0.6346	1.3594		0.1680	0.3575	0.6610	1.1865
200	0.7	1		0.2560	0.5111	0.6571	1.4241		0.2486	0.4934	0.6409	1.3829				0.6649	0.6649
200	0.9	1			0.4825	0.6514	1.1338			0.4639	0.6389	1.1029				0.6625	0.6625
200	1.0	1				0.6372	0.6372				0.6237	0.6237				0.6509	0.6509
300	0.2	1	0.0391	0.2328	0.4955	0.6296	1.3971	0.0045	0.0648	0.4891	0.6116	1.1700	0.0188	0.1659	0.5745	0.6420	1.4011
300	0.3	1	0.0536	0.2386	0.5042	0.6415	1.4379	0.0109	0.0926	0.4968	0.6259	1.2262	0.0192	0.1888	0.5279	0.6529	1.3888
300	0.4	1	0.0745	0.2508	0.5128	0.6478	1.4859	0.0278	0.1278	0.5022	0.6325	1.2902		0.1848	0.4561	0.6584	1.2993
300	0.5	1	0.0781	0.2531	0.5152	0.6513	1.4977	0.0577	0.1636	0.5026	0.6364	1.3603		0.1678	0.3576	0.6620	1.1874
300	0.7	1		0.2527	0.5113	0.6577	1.4217		0.2395	0.4935	0.6413	1.3744				0.6655	0.6655
300	0.9	1			0.4802	0.6513	1.1315			0.4572	0.6391	1.0963				0.6619	0.6619
300	1.0	1				0.6364	0.6364				0.6224	0.6224				0.6495	0.6495
500	0.2	1	0.0427	0.2410	0.5033	0.6372	1.4243	0.0045	0.0714	0.4988	0.6199	1.1946	0.0188	0.1797	0.5757	0.6464	1.4206
500	0.3	1	0.0549	0.2473	0.5103	0.6449	1.4574	0.0103	0.1015	0.5038	0.6306	1.2462	0.0183	0.1908	0.5295	0.6540	1.3927
500	0.4	1	0.0737	0.2541	0.5170	0.6495	1.4943	0.0254	0.1311	0.5073	0.6344	1.2982		0.1857	0.4592	0.6595	1.3045
500	0.5	1	0.0770	0.2536	0.5191	0.6538	1.5035	0.0508	0.1629	0.5066	0.6371	1.3575		0.1647	0.3593	0.6641	1.1881
500	0.7	1		0.2476	0.5111	0.6583	1.4171		0.2271	0.4938	0.6423	1.3632				0.6672	0.6672
500	0.9	1			0.4748	0.6518	1.1267			0.4478	0.6387	1.0865				0.6618	0.6618
500	1.0	1				0.6338	0.6338				0.6217	0.6217				0.6470	0.6470
1000	0.2	1	0.0487	0.2533	0.5086	0.6399	1.4505	0.0045	0.0805	0.5043	0.6239	1.2131	0.0185	0.1869	0.5773	0.6495	1.4321
1000	0.3	1	0.0541	0.2595	0.5169	0.6470	1.4775	0.0096	0.1076	0.5115	0.6337	1.2625	0.0205	0.1941	0.5326	0.6570	1.4042
1000	0.4	1	0.0732	0.2601	0.5220	0.6514	1.5068	0.0207	0.1375	0.5129	0.6372	1.3083		0.1861	0.4634	0.6611	1.3106
1000	0.5	1	0.0730	0.2535	0.5220	0.6552	1.5037		0.1612	0.5120	0.6396	1.3128		0.1594	0.3601	0.6655	1.1850
1000	0.7	1		0.2399	0.5092	0.6588	1.4079		0.2032	0.4925	0.6425	1.3382				0.6673	0.6673
1000	0.9	1			0.4652	0.6507	1.1158			0.4338	0.6359	1.0697				0.6599	0.6599
1000	1.0	1				0.6279	0.6279				0.6142	0.6142				0.6417	0.6417

(a) SoftMax

(b) Garbage

(c) EOS

Table 3: EVM PARAMETER OPTIMIZATION ON P_1 .

λ	κ	ω	10^{-3}	10^{-2}	10^{-1}	1	Σ	10^{-3}	10^{-2}	10^{-1}	1	Σ	10^{-3}	10^{-2}	10^{-1}	1	Σ	
25	0.2	1		0.1221	0.3542	0.6690	1.1453											
25	0.3	1		0.1220	0.3596	0.6697	1.1513		0.1368	0.3771	0.6582	1.1721			0.4484	0.6689	1.1172	
25	0.4	1			0.3643	0.6733	1.0377		0.1334	0.3841	0.6631	1.1806			0.4399	0.6690	1.1089	
25	0.5	1			0.3581	0.6739	1.0320			0.3854	0.6675	1.0529				0.6705	0.6705	
25	0.7	1				0.6741	0.6741			0.3816	0.6719	1.0536				0.6710	0.6710	
25	0.9	1				0.6658	0.6658				0.6765	0.6765				0.6751	0.6751	
25	1.0	1				0.6531	0.6531				0.6669	0.6669				0.6721	0.6721	
50	0.2	1		0.1211	0.3577	0.6712	1.1501		0.1382	0.3839	0.6631	1.1851			0.4485	0.6686	1.1171	
50	0.3	1		0.1218	0.3642	0.6719	1.1579		0.1321	0.3884	0.6667	1.1872			0.4373	0.6701	1.1074	
50	0.4	1			0.3638	0.6732	1.0370		0.1226	0.3877	0.6693	1.1797				0.6711	0.6711	
50	0.5	1			0.3618	0.6747	1.0365			0.3804	0.6733	1.0537				0.6721	0.6721	
50	0.7	1				0.6746	0.6746				0.6758	0.6758				0.6746	0.6746	
50	0.9	1				0.6679	0.6679				0.6696	0.6696				0.6739	0.6739	
50	1.0	1				0.6604	0.6604				0.6584	0.6584				0.6704	0.6704	
75	0.2	1		0.1213	0.3587	0.6696	1.1495		0.1375	0.3864	0.6650	1.1888			0.4484	0.6697	1.1181	
75	0.3	1		0.1215	0.3649	0.6728	1.1592		0.1321	0.3917	0.6675	1.1913			0.4331	0.6704	1.1035	
75	0.4	1			0.3639	0.6726	1.0365		0.1221	0.3873	0.6700	1.1794				0.6708	0.6708	
75	0.5	1			0.3605	0.6739	1.0343			0.3798	0.6733	1.0532				0.6726	0.6726	
75	0.7	1				0.6740	0.6740				0.6761	0.6761				0.6743	0.6743	
75	0.9	1				0.6693	0.6693				0.6700	0.6700				0.6736	0.6736	
75	1.0	1				0.6649	0.6649				0.6611	0.6611				0.6700	0.6700	
100	0.2	1		0.1211	0.3605	0.6711	1.1527		0.1405	0.3875	0.6649	1.1928			0.4485	0.6692	1.1177	
100	0.3	1		0.1202	0.3654	0.6726	1.1582		0.1315	0.3935	0.6679	1.1930			0.4322	0.6700	1.1022	
100	0.4	1			0.3639	0.6732	1.0371		0.1231	0.3876	0.6717	1.1823				0.6708	0.6708	
100	0.5	1			0.3598	0.6740	1.0338			0.3800	0.6722	1.0522				0.6722	0.6722	
100	0.7	1				0.6734	0.6734				0.6761	0.6761				0.6747	0.6747	
100	0.9	1				0.6703	0.6703				0.6712	0.6712				0.6732	0.6732	
100	1.0	1				0.6665	0.6665				0.6620	0.6620				0.6703	0.6703	
150	0.2	1		0.1213	0.3625	0.6711	1.1549		0.1387	0.3873	0.6669	1.1930			0.4493	0.6689	1.1182	
150	0.3	1		0.1199	0.3659	0.6729	1.1586		0.1323	0.3941	0.6699	1.1963			0.4313	0.6705	1.1019	
150	0.4	1			0.3636	0.6723	1.0360		0.1210	0.3882	0.6707	1.1798				0.6708	0.6708	
150	0.5	1			0.3581	0.6732	1.0313			0.3789	0.6728	1.0516				0.6719	0.6719	
150	0.7	1				0.6733	0.6733				0.6757	0.6757				0.6739	0.6739	
150	0.9	1				0.6697	0.6697				0.6725	0.6725				0.6719	0.6719	
150	1.0	1				0.6658	0.6658				0.6633	0.6633				0.6692	0.6692	
200	0.2	1		0.1214	0.3618	0.6711	1.1543		0.1388	0.3905	0.6678	1.1971			0.4480	0.6697	1.1177	
200	0.3	1		0.1196	0.3667	0.6732	1.1595		0.1323	0.3948	0.6707	1.1978			0.4259	0.6707	1.0966	
200	0.4	1			0.3634	0.6733	1.0367		0.1225	0.3879	0.6705	1.1809				0.6711	0.6711	
200	0.5	1			0.3566	0.6737	1.0303			0.3772	0.6733	1.0505				0.6719	0.6719	
200	0.7	1				0.6734	0.6734				0.6762	0.6762				0.6732	0.6732	
200	0.9	1				0.6697	0.6697				0.6719	0.6719				0.6703	0.6703	
200	1.0	1				0.6657	0.6657				0.6632	0.6632				0.6686	0.6686	
300	0.2	1		0.1215	0.3641	0.6717	1.1573		0.1375	0.3938	0.6701	1.2014			0.4467	0.6689	1.1156	
300	0.3	1		0.1226	0.3671	0.6744	1.1642		0.1311	0.3953	0.6711	1.1975			0.4181	0.6708	1.0889	
300	0.4	1			0.3641	0.6748	1.0389		0.1215	0.3877	0.6721	1.1813				0.6719	0.6719	
300	0.5	1			0.3553	0.6750	1.0303			0.3768	0.6737	1.0505				0.6725	0.6725	
300	0.7	1				0.6741	0.6741				0.6766	0.6766				0.6740	0.6740	
300	0.9	1				0.6690	0.6690				0.6729	0.6729				0.6707	0.6707	
300	1.0	1				0.6660	0.6660				0.6647	0.6647				0.6681	0.6681	
500	0.2	1		0.1214	0.3667	0.6718	1.1599		0.1388	0.3976	0.6721	1.2085			0.4426	0.6692	1.1117	
500	0.3	1		0.1206	0.3661	0.6741	1.1609		0.1297	0.3984	0.6734	1.2016			0.4037	0.6703	1.0739	
500	0.4	1			0.3631	0.6748	1.0379			0.3880	0.6744	1.0624				0.6719	0.6719	
500	0.5	1			0.3535	0.6752	1.0288			0.3739	0.6746	1.0484				0.6729	0.6729	
500	0.7	1				0.6752	0.6752				0.6762	0.6762				0.6737	0.6737	
500	0.9	1				0.6690	0.6690				0.6741	0.6741				0.6711	0.6711	
500	1.0	1				0.6660	0.6660				0.6643	0.6643				0.6663	0.6663	
1000	0.2	1		0.1202	0.3678	0.6717	1.1596		0.1400	0.4027	0.6737	1.2164			0.4301	0.6697	1.0998	
1000	0.3	1		0.1159	0.3667	0.6733	1.1559		0.1240	0.3994	0.6741	1.1975			0.3735	0.6701	1.0436	
1000	0.4	1			0.3606	0.6737	1.0343			0.3866	0.6744	1.0610				0.6729	0.6729	
1000	0.5	1			0.3499	0.6752	1.0252			0.3666	0.6741	1.0407				0.6732	0.6732	
1000	0.7	1				0.6736	0.6736				0.6758	0.6758				0.6733	0.6733	
1000	0.9	1				0.6690	0.6690				0.6723	0.6723				0.6697	0.6697	
1000	1.0	1				0.6651	0.6651				0.6653	0.6653				0.6629	0.6629	

(a) SoftMax

(b) Garbage

(c) EOS

Table 4: EVM PARAMETER OPTIMIZATION ON P_2 .

λ	κ	ω	10^{-3}	10^{-2}	10^{-1}	1	Σ	10^{-3}	10^{-2}	10^{-1}	1	Σ	10^{-3}	10^{-2}	10^{-1}	1	Σ
25	0.2	1		0.1067	0.3622	0.6296	1.0985		0.1275	0.3629	0.5937	1.0841			0.5474	0.7487	1.2961
25	0.3	1		0.1191	0.3860	0.7038	1.2089		0.1518	0.4029	0.6607	1.2153			0.5509	0.7576	1.3085
25	0.4	1		0.1252	0.4035	0.7208	1.2494		0.1711	0.4328	0.6918	1.2957			0.5497	0.7600	1.3098
25	0.5	1			0.4171	0.7392	1.1563		0.1830	0.4540	0.7193	1.3564			0.5482	0.7609	1.3091
25	0.7	1			0.4365	0.7617	1.1983			0.4751	0.7588	1.2338				0.7618	0.7618
25	0.9	1				0.7621	0.7621				0.7641	0.7641				0.7602	0.7602
25	1.0	1				0.7368	0.7368				0.7357	0.7357				0.7547	0.7547
50	0.2	1		0.1064	0.3789	0.6610	1.1463		0.1323	0.3954	0.6383	1.1660			0.5492	0.7529	1.3021
50	0.3	1		0.1204	0.3961	0.7239	1.2404		0.1537	0.4226	0.6989	1.2752			0.5510	0.7597	1.3107
50	0.4	1		0.1257	0.4094	0.7386	1.2737		0.1708	0.4429	0.7211	1.3349			0.5500	0.7609	1.3109
50	0.5	1		0.1337	0.4196	0.7507	1.3040		0.1837	0.4581	0.7396	1.3814			0.5465	0.7623	1.3088
50	0.7	1			0.4360	0.7655	1.2015			0.4753	0.7654	1.2406				0.7631	0.7631
50	0.9	1				0.7642	0.7642				0.7658	0.7658				0.7613	0.7613
50	1.0	1				0.7428	0.7428				0.7411	0.7411				0.7565	0.7565
75	0.2	1		0.1086	0.3835	0.6782	1.1703		0.1300	0.4062	0.6605	1.1968			0.5506	0.7551	1.3056
75	0.3	1		0.1219	0.3985	0.7340	1.2544		0.1532	0.4283	0.7148	1.2963			0.5518	0.7605	1.3122
75	0.4	1		0.1257	0.4102	0.7453	1.2811		0.1708	0.4446	0.7328	1.3482			0.5497	0.7619	1.3116
75	0.5	1		0.1329	0.4213	0.7552	1.3094		0.1833	0.4584	0.7481	1.3898			0.5458	0.7627	1.3085
75	0.7	1			0.4360	0.7668	1.2028			0.4755	0.7671	1.2426				0.7634	0.7634
75	0.9	1				0.7646	0.7646				0.7666	0.7666				0.7620	0.7620
75	1.0	1				0.7434	0.7434				0.7423	0.7423				0.7569	0.7569
100	0.2	1		0.1115	0.3862	0.6898	1.1875		0.1262	0.4104	0.6744	1.2110			0.5508	0.7562	1.3070
100	0.3	1		0.1222	0.4005	0.7391	1.2618		0.1523	0.4296	0.7237	1.3056			0.5526	0.7606	1.3133
100	0.4	1		0.1256	0.4128	0.7491	1.2876		0.1703	0.4449	0.7391	1.3543			0.5491	0.7621	1.3112
100	0.5	1		0.1323	0.4216	0.7575	1.3113		0.1822	0.4583	0.7528	1.3933			0.5442	0.7629	1.3071
100	0.7	1			0.4357	0.7672	1.2028			0.4758	0.7685	1.2443				0.7637	0.7637
100	0.9	1				0.7650	0.7650				0.7666	0.7666				0.7618	0.7618
100	1.0	1				0.7439	0.7439				0.7429	0.7429				0.7569	0.7569
150	0.2	1		0.1122	0.3881	0.7060	1.2062		0.1227	0.4140	0.6915	1.2282			0.5525	0.7581	1.3105
150	0.3	1		0.1209	0.4008	0.7453	1.2670		0.1451	0.4299	0.7339	1.3090			0.5528	0.7613	1.3141
150	0.4	1		0.1262	0.4142	0.7533	1.2938		0.1701	0.4450	0.7465	1.3616			0.5482	0.7626	1.3108
150	0.5	1			0.4223	0.7603	1.1825		0.1825	0.4592	0.7563	1.3980			0.5416	0.7634	1.3050
150	0.7	1			0.4349	0.7684	1.2033			0.4762	0.7691	1.2452				0.7643	0.7643
150	0.9	1				0.7647	0.7647				0.7668	0.7668				0.7621	0.7621
150	1.0	1				0.7436	0.7436				0.7425	0.7425				0.7572	0.7572
200	0.2	1		0.1129	0.3904	0.7156	1.2188		0.1182	0.4154	0.7030	1.2367			0.5536	0.7593	1.3129
200	0.3	1		0.1205	0.4012	0.7481	1.2698		0.1402	0.4304	0.7392	1.3097			0.5527	0.7617	1.3144
200	0.4	1		0.1269	0.4141	0.7558	1.2967		0.1707	0.4449	0.7497	1.3653			0.5479	0.7633	1.3111
200	0.5	1			0.4229	0.7617	1.1847		0.1824	0.4596	0.7587	1.4006			0.5390	0.7636	1.3027
200	0.7	1			0.4348	0.7690	1.2038			0.4763	0.7694	1.2456				0.7647	0.7647
200	0.9	1				0.7647	0.7647				0.7664	0.7664				0.7624	0.7624
200	1.0	1				0.7436	0.7436				0.7405	0.7405				0.7566	0.7566
300	0.2	1		0.1115	0.3904	0.7275	1.2294		0.1035	0.4174	0.7158	1.2368			0.5558	0.7611	1.3169
300	0.3	1		0.1206	0.4012	0.7516	1.2734		0.1355	0.4320	0.7452	1.3128			0.5535	0.7627	1.3162
300	0.4	1		0.1264	0.4141	0.7587	1.2993		0.1710	0.4467	0.7543	1.3720			0.5460	0.7641	1.3101
300	0.5	1			0.4236	0.7641	1.1877		0.1820	0.4600	0.7610	1.4030			0.5350	0.7643	1.2994
300	0.7	1			0.4341	0.7695	1.2036			0.4754	0.7701	1.2455				0.7653	0.7653
300	0.9	1				0.7650	0.7650				0.7658	0.7658				0.7622	0.7622
300	1.0	1				0.7422	0.7422				0.7378	0.7378				0.7557	0.7557
500	0.2	1		0.1105	0.3900	0.7398	1.2403		0.0859	0.4191	0.7316	1.2365			0.5573	0.7620	1.3192
500	0.3	1		0.1208	0.4019	0.7558	1.2784		0.1292	0.4334	0.7506	1.3132			0.5538	0.7636	1.3175
500	0.4	1		0.1255	0.4142	0.7605	1.3001		0.1735	0.4477	0.7573	1.3786			0.5432	0.7643	1.3075
500	0.5	1			0.4239	0.7658	1.1897		0.1824	0.4602	0.7635	1.4061			0.5284	0.7653	1.2936
500	0.7	1			0.4321	0.7707	1.2028			0.4740	0.7709	1.2448				0.7656	0.7656
500	0.9	1				0.7628	0.7628				0.7643	0.7643				0.7617	0.7617
500	1.0	1				0.7373	0.7373				0.7317	0.7317				0.7534	0.7534
1000	0.2	1		0.1079	0.3859	0.7495	1.2433		0.0689	0.4171	0.7390	1.2250			0.5602	0.7626	1.3228
1000	0.3	1		0.1208	0.4022	0.7571	1.2801		0.1232	0.4347	0.7519	1.3098			0.5530	0.7635	1.3165
1000	0.4	1		0.1278	0.4153	0.7626	1.3057		0.1742	0.4473	0.7599	1.3814			0.5355	0.7650	1.3005
1000	0.5	1			0.4237	0.7674	1.1912		0.1785	0.4607	0.7657	1.4049				0.7655	0.7655
1000	0.7	1			0.4292	0.7715	1.2008			0.4709	0.7711	1.2420				0.7657	0.7657
1000	0.9	1				0.7604	0.7604				0.7614	0.7614				0.7604	0.7604
1000	1.0	1				0.7293	0.7293				0.7196	0.7196				0.7498	0.7498

(a) SoftMax

(b) Garbage

(c) EOS

Table 5: EVM PARAMETER OPTIMIZATION ON P_3 .

λ	κ	α	10^{-3}	10^{-2}	10^{-1}	1	Σ	10^{-3}	10^{-2}	10^{-1}	1	Σ	10^{-3}	10^{-2}	10^{-1}	1	Σ
10	1.5	2		0.1908	0.4235	0.6540	1.2683		0.1943	0.4129	0.6397	1.2469	0.2954	0.5759	0.6601	0.6616	2.1931
10	1.5	3		0.1911	0.4237	0.6541	1.2689		0.1943	0.4129	0.6398	1.2469	0.2955	0.5760	0.6602	0.6617	2.1934
10	1.5	5		0.1911	0.4232	0.6540	1.2683		0.1944	0.4124	0.6398	1.2466	0.2950	0.5748	0.6601	0.6617	2.1917
10	1.5	10		0.1911	0.4226	0.6541	1.2678		0.1933	0.4119	0.6399	1.2451	0.2943	0.5747	0.6602	0.6617	2.1909
10	1.7	2		0.1908	0.4235	0.6537	1.2679		0.1944	0.4125	0.6397	1.2466	0.2954	0.5761	0.6602	0.6618	2.1935
10	1.7	3		0.1911	0.4235	0.6537	1.2683		0.1944	0.4125	0.6398	1.2467	0.2954	0.5761	0.6602	0.6618	2.1935
10	1.7	5		0.1911	0.4235	0.6537	1.2683		0.1945	0.4126	0.6398	1.2468	0.2954	0.5760	0.6602	0.6618	2.1934
10	1.7	10		0.1911	0.4229	0.6537	1.2677		0.1945	0.4126	0.6398	1.2468	0.2953	0.5749	0.6602	0.6618	2.1923
10	2.0	2		0.1908	0.4232	0.6537	1.2677		0.1944	0.4126	0.6396	1.2465	0.2954	0.5761	0.6602	0.6618	2.1936
10	2.0	3		0.1908	0.4232	0.6537	1.2677		0.1944	0.4126	0.6396	1.2465	0.2954	0.5761	0.6602	0.6618	2.1936
10	2.0	5		0.1908	0.4232	0.6537	1.2677		0.1944	0.4126	0.6396	1.2465	0.2954	0.5761	0.6602	0.6618	2.1936
10	2.0	10		0.1908	0.4232	0.6537	1.2677		0.1944	0.4125	0.6396	1.2465	0.2954	0.5759	0.6602	0.6618	2.1934
10	2.3	2		0.1908	0.4232	0.6537	1.2677		0.1944	0.4126	0.6396	1.2465	0.2954	0.5761	0.6602	0.6618	2.1936
10	2.3	3		0.1908	0.4232	0.6537	1.2677		0.1944	0.4126	0.6396	1.2465	0.2954	0.5761	0.6602	0.6618	2.1936
10	2.3	5		0.1908	0.4232	0.6537	1.2677		0.1944	0.4126	0.6396	1.2465	0.2954	0.5761	0.6602	0.6618	2.1936
10	2.3	10		0.1908	0.4232	0.6537	1.2677		0.1944	0.4126	0.6396	1.2465	0.2954	0.5760	0.6602	0.6618	2.1935
100	1.5	2		0.1954	0.4340	0.6569	1.2862		0.2007	0.4212	0.6405	1.2624	0.2956	0.5823	0.6604	0.6616	2.1999
100	1.5	3		0.1924	0.4334	0.6582	1.2839		0.1991	0.4191	0.6425	1.2607	0.2962	0.5849	0.6624	0.6639	2.2074
100	1.5	5		0.1884	0.4286	0.6592	1.2761		0.1956	0.4156	0.6439	1.2551	0.2862	0.5854	0.6636	0.6649	2.2001
100	1.5	10		0.2051	0.4372	0.6595	1.3019		0.1976	0.4169	0.6444	1.2589	0.3477	0.5970	0.6585	0.6654	2.2686
100	1.7	2		0.1916	0.4284	0.6552	1.2753		0.1957	0.4160	0.6406	1.2523	0.2954	0.5792	0.6609	0.6623	2.1979
100	1.7	3		0.1913	0.4286	0.6564	1.2763		0.1957	0.4154	0.6414	1.2525	0.2946	0.5802	0.6619	0.6633	2.2000
100	1.7	5		0.1890	0.4266	0.6569	1.2724		0.1940	0.4127	0.6417	1.2484	0.2917	0.5788	0.6620	0.6635	2.1959
100	1.7	10		0.1872	0.4250	0.6569	1.2690		0.1939	0.4107	0.6417	1.2463	0.2941	0.5838	0.6619	0.6634	2.2032
100	2.0	2		0.1911	0.4253	0.6548	1.2711		0.1944	0.4137	0.6399	1.2480	0.2953	0.5778	0.6605	0.6620	2.1956
100	2.0	3		0.1905	0.4259	0.6550	1.2713		0.1948	0.4134	0.6402	1.2484	0.2958	0.5782	0.6605	0.6621	2.1967
100	2.0	5		0.1908	0.4250	0.6550	1.2708		0.1941	0.4127	0.6403	1.2471	0.2944	0.5761	0.6607	0.6623	2.1935
100	2.0	10		0.1899	0.4236	0.6550	1.2685		0.1932	0.4109	0.6404	1.2446	0.2927	0.5749	0.6607	0.6623	2.1906
100	2.3	2		0.1907	0.4240	0.6541	1.2688		0.1945	0.4128	0.6398	1.2471	0.2954	0.5764	0.6600	0.6615	2.1933
100	2.3	3		0.1908	0.4242	0.6541	1.2690		0.1945	0.4131	0.6398	1.2474	0.2955	0.5761	0.6600	0.6615	2.1933
100	2.3	5		0.1908	0.4241	0.6541	1.2690		0.1947	0.4127	0.6399	1.2472	0.2951	0.5767	0.6601	0.6616	2.1935
100	2.3	10		0.1905	0.4236	0.6541	1.2683		0.1949	0.4126	0.6399	1.2473	0.2946	0.5756	0.6602	0.6618	2.1922
250	1.5	2		0.2065	0.4551	0.6542	1.3157		0.2148	0.4375	0.6390	1.2913	0.3147	0.5806	0.6583	0.6596	2.2132
250	1.5	3		0.2119	0.4547	0.6588	1.3255		0.2151	0.4394	0.6427	1.2972	0.3164	0.5900	0.6624	0.6638	2.2326
250	1.5	5		0.2109	0.4524	0.6624	1.3257		0.2146	0.4375	0.6472	1.2993	0.3370	0.6012	0.6638	0.6661	2.2681
250	1.5	10	0.0847	0.2401	0.4964	0.6637	1.4850		0.2308	0.4539	0.6484	1.3331	0.3392	0.5564	0.6090	0.6685	2.1731
250	1.7	2		0.2016	0.4427	0.6570	1.3013		0.2063	0.4270	0.6397	1.2731	0.2995	0.5792	0.6605	0.6618	2.2010
250	1.7	3		0.2014	0.4435	0.6602	1.3050		0.2056	0.4269	0.6432	1.2756	0.3029	0.5840	0.6640	0.6655	2.2165
250	1.7	5		0.2019	0.4385	0.6616	1.3020		0.2007	0.4236	0.6449	1.2692	0.2901	0.5894	0.6641	0.6655	2.2090
250	1.7	10		0.2219	0.4564	0.6620	1.3403		0.2062	0.4280	0.6460	1.2802	0.3608	0.5994	0.6557	0.6666	2.2824
250	2.0	2		0.1968	0.4320	0.6562	1.2850		0.2011	0.4188	0.6404	1.2603	0.2977	0.5783	0.6603	0.6617	2.1980
250	2.0	3		0.1953	0.4334	0.6586	1.2872		0.2006	0.4177	0.6420	1.2603	0.2947	0.5802	0.6620	0.6635	2.2003
250	2.0	5		0.1944	0.4316	0.6590	1.2850		0.2001	0.4166	0.6426	1.2593	0.2895	0.5807	0.6624	0.6639	2.1965
250	2.0	10		0.1941	0.4296	0.6593	1.2830		0.1983	0.4153	0.6432	1.2568	0.3020	0.5866	0.6626	0.6642	2.2153
250	2.3	2		0.1915	0.4288	0.6551	1.2753		0.1955	0.4147	0.6400	1.2501	0.2968	0.5784	0.6606	0.6620	2.1978
250	2.3	3		0.1925	0.4293	0.6555	1.2772		0.1956	0.4146	0.6407	1.2509	0.2951	0.5799	0.6611	0.6627	2.1988
250	2.3	5		0.1924	0.4284	0.6562	1.2771		0.1953	0.4141	0.6411	1.2505	0.2916	0.5803	0.6614	0.6629	2.1964
250	2.3	10		0.1910	0.4258	0.6565	1.2733		0.1946	0.4123	0.6412	1.2480	0.2905	0.5785	0.6614	0.6629	2.1933
500	1.5	2		0.2273	0.4652	0.6409	1.3334		0.2383	0.4484	0.6272	1.3138	0.3309	0.5872	0.6435	0.6445	2.2061
500	1.5	3		0.2367	0.4802	0.6472	1.3641		0.2454	0.4617	0.6357	1.3428	0.3408	0.5985	0.6483	0.6495	2.2371
500	1.5	5		0.2544	0.4963	0.6570	1.4077		0.2511	0.4734	0.6440	1.3685	0.3607	0.6021	0.6445	0.6566	2.2638
500	1.5	10	0.1131	0.2568	0.4913	0.6612	1.5225	0.0929	0.2440	0.4581	0.6492	1.4442	0.2477	0.3827	0.4342	0.6631	1.7277
500	1.7	2		0.2183	0.4588	0.6482	1.3253		0.2244	0.4406	0.6354	1.3005	0.3144	0.5773	0.6529	0.6542	2.1988
500	1.7	3		0.2288	0.4649	0.6552	1.3490		0.2301	0.4463	0.6411	1.3175	0.3262	0.5897	0.6577	0.6591	2.2327
500	1.7	5		0.2325	0.4678	0.6618	1.3621		0.2286	0.4476	0.6457	1.3218	0.3478	0.6043	0.6607	0.6632	2.2760
500	1.7	10	0.1006	0.2567	0.5093	0.6644	1.5310	0.0985	0.2535	0.4718	0.6482	1.4720	0.3191	0.5237	0.5777	0.6670	2.0874
500	2.0	2		0.2070	0.4468	0.6553	1.3091		0.2120	0.4285	0.6382	1.2787	0.3023	0.5774	0.6583	0.6596	2.1976
500	2.0	3		0.2119	0.4502	0.6599	1.3220		0.2156	0.4318	0.6419	1.2893	0.3124	0.5822	0.6626	0.6642	2.2215
500	2.0	5		0.2139	0.4480	0.6616	1.3235		0.2146	0.4307	0.6450	1.2903	0.3041	0.5896	0.6635	0.6649	2.2222
500	2.0	10		0.2348	0.4701	0.6627	1.3675		0.2144	0.4360	0.6457	1.2961	0.3678	0.6003	0.6525	0.6660	2.2667
500	2.3	2		0.2019	0.4389	0.6567	1.2974		0.2055	0.4216	0.6401	1.2672	0.2971	0.5784	0.6593	0.6606	2.1954
500	2.3	3		0.2043	0.4418	0.6599	1.3060		0.2094	0.4243	0.6419	1.2755	0.2938	0.5815	0.6623	0.6638	2.2014
500	2.3	5		0.2063	0.4402	0.6604	1.3069		0.2065	0.4222	0.6432	1.2719	0.2931	0.5844	0.6634	0.6649	2.2059
500	2.3	10		0.2084	0.4415	0.6608	1.3107		0.2076	0.4210	0.6438	1.2724	0.3344	0.5907	0.6633	0.6653	2.2537
750	1.5	2	0.0581	0.2356	0.4491	0.6165	1.3592	0.0772	0.2473	0.4384	0.6074	1.3703	0.3239	0.5765	0.6232	0.6243	2.1479
750	1.5	3	0.0768	0.2601	0.4919	0.6246	1.4533		0.2611	0.4747	0.6167	1.3525	0.3382	0.5976	0.6292	0.6304	2.1953
750	1.5	5	0.0910	0.2755	0.5262	0.6382	1.5309	0.0971	0.2902	0.5089	0.6300	1.5262	0.3574	0.5702	0.6079	0.6394	2.1749
750	1.5	10	0.1093	0.2442	0.4616	0.6530	1.4681	0.0852	0.2								

λ	κ	α	10^{-3}	10^{-2}	10^{-1}	1	Σ	10^{-3}	10^{-2}	10^{-1}	1	Σ	10^{-3}	10^{-2}	10^{-1}	1	Σ
10	1.5	2		0.1065	0.3351	0.6715	1.1131		0.1549	0.3566	0.6582	1.1697		0.3230	0.5898	0.6645	1.5772
10	1.5	3		0.1083	0.3346	0.6719	1.1148		0.1549	0.3569	0.6586	1.1704		0.3278	0.5898	0.6658	1.5835
10	1.5	5		0.1071	0.3344	0.6718	1.1134		0.1535	0.3566	0.6591	1.1692		0.3278	0.5901	0.6657	1.5836
10	1.5	10		0.1070	0.3342	0.6718	1.1130		0.1524	0.3544	0.6591	1.1658		0.3188	0.5818	0.6663	1.5669
10	1.7	2		0.1065	0.3351	0.6715	1.1131		0.1549	0.3567	0.6585	1.1701		0.3221	0.5890	0.6651	1.5763
10	1.7	3		0.1070	0.3340	0.6719	1.1130		0.1557	0.3558	0.6589	1.1704		0.3267	0.5897	0.6657	1.5821
10	1.7	5		0.1081	0.3344	0.6718	1.1143		0.1553	0.3559	0.6585	1.1697		0.3288	0.5901	0.6672	1.5861
10	1.7	10		0.1088	0.3347	0.6719	1.1154		0.1548	0.3560	0.6584	1.1692		0.3306	0.5880	0.6668	1.5854
10	2.0	2		0.1065	0.3351	0.6719	1.1135		0.1549	0.3563	0.6585	1.1697		0.3220	0.5897	0.6645	1.5761
10	2.0	3		0.1069	0.3344	0.6719	1.1132		0.1550	0.3559	0.6585	1.1694		0.3235	0.5891	0.6647	1.5774
10	2.0	5		0.1070	0.3343	0.6719	1.1132		0.1550	0.3559	0.6585	1.1694		0.3253	0.5896	0.6660	1.5808
10	2.0	10		0.1073	0.3347	0.6719	1.1139		0.1552	0.3555	0.6585	1.1692		0.3324	0.5891	0.6667	1.5882
10	2.3	2		0.1065	0.3351	0.6717	1.1132		0.1549	0.3562	0.6586	1.1697		0.3220	0.5893	0.6645	1.5757
10	2.3	3		0.1065	0.3347	0.6717	1.1128		0.1549	0.3562	0.6586	1.1697		0.3242	0.5900	0.6661	1.5803
10	2.3	5		0.1069	0.3346	0.6718	1.1132		0.1546	0.3559	0.6586	1.1692		0.3230	0.5894	0.6665	1.5789
10	2.3	10		0.1069	0.3347	0.6718	1.1134		0.1549	0.3559	0.6585	1.1693		0.3257	0.5894	0.6663	1.5814
100	1.5	2		0.1078	0.3378	0.6692	1.1148		0.1539	0.3598	0.6591	1.1728		0.3153	0.5839	0.6550	1.5543
100	1.5	3		0.1065	0.3361	0.6730	1.1156		0.1520	0.3617	0.6635	1.1772		0.3243	0.5817	0.6535	1.5595
100	1.5	5		0.1026	0.3322	0.6737	1.1085		0.1506	0.3645	0.6660	1.1811		0.3171	0.5602	0.6550	1.5324
100	1.5	10		0.0793	0.3301	0.6746	1.0840		0.1105	0.3293	0.6668	1.1066	0.0717	0.2832	0.5075	0.6599	1.5223
100	1.7	2		0.1080	0.3364	0.6712	1.1156		0.1541	0.3583	0.6591	1.1714		0.3167	0.5862	0.6585	1.5615
100	1.7	3		0.1074	0.3358	0.6732	1.1164		0.1535	0.3594	0.6615	1.1744		0.3250	0.5861	0.6588	1.5699
100	1.7	5		0.1070	0.3311	0.6744	1.1125		0.1507	0.3599	0.6640	1.1747		0.3210	0.5705	0.6589	1.5504
100	1.7	10		0.0977	0.3432	0.6743	1.1152		0.1357	0.3437	0.6645	1.1438	0.0756	0.2910	0.5206	0.6636	1.5508
100	2.0	2		0.1063	0.3358	0.6714	1.1135		0.1539	0.3574	0.6599	1.1712		0.3178	0.5879	0.6613	1.5670
100	2.0	3		0.1070	0.3351	0.6726	1.1148		0.1557	0.3583	0.6613	1.1752		0.3249	0.5886	0.6613	1.5748
100	2.0	5		0.1056	0.3318	0.6736	1.1110		0.1548	0.3587	0.6618	1.1752		0.3216	0.5793	0.6622	1.5631
100	2.0	10		0.1049	0.3353	0.6728	1.1130		0.1513	0.3573	0.6620	1.1705		0.3007	0.5450	0.6640	1.5097
100	2.3	2		0.1063	0.3353	0.6717	1.1132		0.1548	0.3571	0.6595	1.1714		0.3191	0.5879	0.6633	1.5703
100	2.3	3		0.1081	0.3350	0.6722	1.1153		0.1561	0.3571	0.6596	1.1729		0.3254	0.5893	0.6645	1.5792
100	2.3	5		0.1055	0.3339	0.6723	1.1117		0.1561	0.3573	0.6606	1.1740		0.3243	0.5849	0.6645	1.5736
100	2.3	10		0.1070	0.3314	0.6721	1.1105		0.1556	0.3570	0.6604	1.1730		0.3077	0.5608	0.6639	1.5324
250	1.5	2		0.1105	0.3463	0.6579	1.1148		0.1516	0.3667	0.6507	1.1690		0.3127	0.5734	0.6409	1.5270
250	1.5	3		0.1146	0.3483	0.6642	1.1271		0.1537	0.3717	0.6604	1.1858		0.3210	0.5673	0.6431	1.5314
250	1.5	5		0.1123	0.3559	0.6704	1.1386		0.1531	0.3814	0.6654	1.1999	0.0886	0.3015	0.5234	0.6420	1.5555
250	1.5	10	0.0209	0.0973	0.3116	0.6748	1.1047	0.0305	0.1012	0.3122	0.6679	1.1117	0.0689	0.2539	0.4488	0.6506	1.4222
250	1.7	2		0.1105	0.3443	0.6668	1.1215		0.1521	0.3631	0.6556	1.1708		0.3142	0.5781	0.6476	1.5399
250	1.7	3		0.1154	0.3423	0.6715	1.1293		0.1517	0.3675	0.6624	1.1816		0.3236	0.5763	0.6487	1.5486
250	1.7	5		0.1048	0.3434	0.6736	1.1218		0.1574	0.3720	0.6665	1.1959	0.0879	0.3074	0.5347	0.6506	1.5807
250	1.7	10	0.0249	0.0973	0.3349	0.6773	1.1344	0.0363	0.1114	0.3347	0.6676	1.1501	0.0698	0.2632	0.4659	0.6574	1.4563
250	2.0	2		0.1084	0.3393	0.6692	1.1168		0.1550	0.3602	0.6567	1.1699		0.3162	0.5842	0.6541	1.5544
250	2.0	3		0.1116	0.3387	0.6725	1.1228		0.1557	0.3630	0.6613	1.1800		0.3260	0.5822	0.6552	1.5634
250	2.0	5		0.1094	0.3371	0.6743	1.1207		0.1568	0.3649	0.6640	1.1858	0.0815	0.3167	0.5538	0.6574	1.6095
250	2.0	10		0.0984	0.3509	0.6748	1.1242		0.1347	0.3498	0.6642	1.1487	0.0720	0.2762	0.4862	0.6621	1.4964
250	2.3	2		0.1098	0.3371	0.6704	1.1172		0.1531	0.3595	0.6564	1.1690		0.3170	0.5861	0.6582	1.5613
250	2.3	3		0.1084	0.3369	0.6747	1.1200		0.1556	0.3614	0.6595	1.1765		0.3267	0.5849	0.6574	1.5689
250	2.3	5		0.1096	0.3340	0.6736	1.1172		0.1574	0.3623	0.6622	1.1819		0.3184	0.5664	0.6595	1.5443
250	2.3	10		0.1080	0.3394	0.6733	1.1207		0.1512	0.3598	0.6621	1.1730	0.0749	0.2810	0.5069	0.6642	1.5270
500	1.5	2		0.1163	0.3484	0.6370	1.1017		0.1519	0.3717	0.6329	1.1564		0.3079	0.5641	0.6287	1.5007
500	1.5	3		0.1184	0.3588	0.6469	1.1240		0.1586	0.3854	0.6445	1.1885	0.0814	0.3166	0.5472	0.6289	1.5741
500	1.5	5		0.1246	0.3714	0.6542	1.1502		0.1591	0.3902	0.6596	1.2089	0.0873	0.2775	0.4780	0.6260	1.4689
500	1.5	10	0.0252	0.1001	0.3152	0.6686	1.1091	0.0206	0.0955	0.2968	0.6665	1.0795	0.0663	0.2244	0.3873	0.6347	1.3127
500	1.7	2		0.1164	0.3486	0.6501	1.1150		0.1517	0.3692	0.6440	1.1649		0.3095	0.5677	0.6344	1.5116
500	1.7	3		0.1210	0.3520	0.6599	1.1329		0.1567	0.3797	0.6546	1.1910	0.0846	0.3198	0.5598	0.6375	1.6016
500	1.7	5		0.1203	0.3646	0.6656	1.1505		0.1525	0.3876	0.6642	1.2043	0.0908	0.2845	0.4950	0.6326	1.5029
500	1.7	10	0.0361	0.1049	0.3159	0.6750	1.1319	0.0238	0.1024	0.3119	0.6687	1.1069	0.0645	0.2323	0.4014	0.6445	1.3427
500	2.0	2		0.1149	0.3466	0.6597	1.1213		0.1512	0.3643	0.6512	1.1667		0.3122	0.5745	0.6413	1.5280
500	2.0	3		0.1200	0.3470	0.6667	1.1337		0.1546	0.3736	0.6604	1.1887	0.0898	0.3218	0.5689	0.6433	1.6239
500	2.0	5		0.1189	0.3555	0.6721	1.1465		0.1556	0.3787	0.6663	1.2006	0.0936	0.2882	0.5172	0.6448	1.5437
500	2.0	10	0.0284	0.1156	0.3404	0.6747	1.1591	0.0378	0.1134	0.3367	0.6671	1.1549	0.0623	0.2407	0.4210	0.6542	1.3782
500	2.3	2		0.1120	0.3434	0.6628	1.1182		0.1521	0.3613	0.6560	1.1694		0.3133	0.5771	0.6458	1.5361
500	2.3	3		0.1161	0.3425	0.6696	1.1282		0.1531	0.3689	0.6611	1.1831		0.3236	0.5756	0.6474	1.5467
500	2.3	5		0.1182	0.3462	0.6740	1.1384		0.1553	0.3721	0.6640	1.1914	0.0973	0.3009	0.5289	0.6524	1.5796
500	2.3	10		0.1062	0.3602	0.6747	1.1411		0.1292	0.3614	0.6632	1.1538	0.0652	0.2470	0.4438	0.6585	1.4145
750	1.5	2		0.1188	0.3491	0.6189	1.0868		0.1553	0.3742	0.6184	1.1478	0.0887	0.3099	0.5565	0.6213	1.5764
750	1.5	3		0.1168	0.3649	0.6272	1.1089		0.1589	0.3934	0.6297	1.1820	0.0836	0.3055	0.5324	0.6163	1.5378
750	1.5	5		0.1287	0.3735	0.6380	1.1402	0.0518	0.1564	0.3876	0.6455	1.2413	0.0800	0.2611	0.4475	0.6210	1.4096
750	1.5	10	0.0233	0.0872	0.3025	0.6609	1.0738	0.0159	0.0890	0.2767	0.6633	1.0450	0.0580	0.1980	0.3465	0.6285	1.2309
750	1.7	2		0.1161	0.3475	0.6329	1.0965		0.1527	0.3695	0.6289	1.1510	0.0905	0.3099	0.5606	0.6262	1.5873
750	1.7	3</															

λ	κ	α	10^{-3}	10^{-2}	10^{-1}	1	Σ	10^{-3}	10^{-2}	10^{-1}	1	Σ	10^{-3}	10^{-2}	10^{-1}	1	Σ	
10	1.5	2			0.4379	0.7758	1.2137			0.5078	0.7714	1.2792		0.4044	0.6621	0.7587	1.8252	
10	1.5	3			0.4379	0.7759	1.2138			0.5077	0.7715	1.2792		0.4054	0.6624	0.7585	1.8263	
10	1.5	5			0.4371	0.7760	1.2132			0.5077	0.7715	1.2792		0.4042	0.6622	0.7586	1.8250	
10	1.5	10			0.4368	0.7761	1.2129			0.5080	0.7716	1.2795		0.4044	0.6639	0.7587	1.8270	
10	1.7	2			0.4377	0.7757	1.2134			0.5078	0.7712	1.2790		0.4045	0.6618	0.7596	1.8258	
10	1.7	3			0.4378	0.7757	1.2135			0.5078	0.7713	1.2791		0.4049	0.6618	0.7593	1.8260	
10	1.7	5			0.4379	0.7757	1.2136			0.5079	0.7713	1.2792		0.4061	0.6618	0.7591	1.8270	
10	1.7	10			0.4378	0.7757	1.2135			0.5079	0.7713	1.2792		0.4033	0.6619	0.7590	1.8241	
10	2.0	2			0.4377	0.7757	1.2134			0.5078	0.7712	1.2790		0.4045	0.6617	0.7595	1.8257	
10	2.0	3			0.4377	0.7757	1.2134			0.5078	0.7712	1.2790		0.4050	0.6616	0.7596	1.8261	
10	2.0	5			0.4378	0.7757	1.2134			0.5078	0.7712	1.2790		0.4046	0.6617	0.7596	1.8258	
10	2.0	10			0.4378	0.7757	1.2135			0.5078	0.7712	1.2790		0.4048	0.6616	0.7597	1.8260	
10	2.3	2			0.4377	0.7756	1.2134			0.5078	0.7713	1.2791		0.4046	0.6615	0.7596	1.8256	
10	2.3	3			0.4378	0.7757	1.2135			0.5078	0.7713	1.2791		0.4047	0.6615	0.7596	1.8258	
10	2.3	5			0.4377	0.7757	1.2134			0.5078	0.7713	1.2791		0.4049	0.6616	0.7595	1.8259	
10	2.3	10			0.4377	0.7757	1.2134			0.5078	0.7713	1.2791		0.4050	0.6617	0.7595	1.8262	
100	1.5	2			0.4393	0.7778	1.2172			0.5093	0.7730	1.2823		0.4007	0.6614	0.7519	1.8140	
100	1.5	3			0.4383	0.7785	1.2168			0.5114	0.7738	1.2852		0.4030	0.6626	0.7528	1.8184	
100	1.5	5			0.4378	0.7790	1.2169			0.5116	0.7741	1.2857		0.4033	0.6606	0.7543	1.8182	
100	1.5	10			0.4282	0.7793	1.2075			0.5066	0.7745	1.2811		0.3857	0.6245	0.7561	1.7663	
100	1.7	2			0.4385	0.7771	1.2156			0.5088	0.7728	1.2815		0.4011	0.6613	0.7554	1.8178	
100	1.7	3			0.4388	0.7777	1.2165			0.5097	0.7730	1.2828		0.4021	0.6622	0.7572	1.8215	
100	1.7	5			0.4373	0.7778	1.2151			0.5097	0.7733	1.2829		0.4020	0.6626	0.7575	1.8221	
100	1.7	10			0.4365	0.7780	1.2145			0.5100	0.7733	1.2833		0.3986	0.6428	0.7585	1.8000	
100	2.0	2			0.4378	0.7764	1.2142			0.5082	0.7715	1.2798		0.4015	0.6622	0.7582	1.8219	
100	2.0	3			0.4376	0.7765	1.2141			0.5086	0.7717	1.2804		0.4025	0.6626	0.7587	1.8238	
100	2.0	5			0.4370	0.7765	1.2134			0.5088	0.7718	1.2806		0.4040	0.6641	0.7585	1.8266	
100	2.0	10			0.4371	0.7766	1.2137			0.5088	0.7719	1.2808		0.4018	0.6572	0.7591	1.8180	
100	2.3	2			0.4379	0.7758	1.2137			0.5079	0.7713	1.2792		0.4022	0.6629	0.7584	1.8235	
100	2.3	3			0.4378	0.7758	1.2136			0.5080	0.7714	1.2794		0.4028	0.6630	0.7590	1.8249	
100	2.3	5			0.4377	0.7758	1.2135			0.5083	0.7714	1.2797		0.4037	0.6632	0.7591	1.8260	
100	2.3	10			0.4374	0.7758	1.2132			0.5083	0.7714	1.2797		0.4029	0.6630	0.7592	1.8251	
250	1.5	2			0.4414	0.7736	1.2149			0.5104	0.7724	1.2828		0.3994	0.6563	0.7385	1.7942	
250	1.5	3			0.4415	0.7765	1.2180			0.5138	0.7744	1.2882		0.4066	0.6603	0.7402	1.8071	
250	1.5	5			0.4396	0.7797	1.2193			0.5150	0.7760	1.2911		0.3998	0.6466	0.7422	1.7885	
250	1.5	10			0.3824	0.7811	1.1635			0.4818	0.7770	1.2588		0.1493	0.3515	0.5752	0.7457	1.8217
250	1.7	2			0.4406	0.7768	1.2175			0.5105	0.7731	1.2837		0.3989	0.6581	0.7453	1.8023	
250	1.7	3			0.4396	0.7784	1.2180			0.5130	0.7749	1.2880		0.4060	0.6613	0.7477	1.8150	
250	1.7	5			0.4378	0.7801	1.2179			0.5142	0.7754	1.2897		0.4023	0.6538	0.7496	1.8057	
250	1.7	10			0.4277	0.7802	1.2079			0.5086	0.7758	1.2844		0.1542	0.3654	0.5957	0.7533	1.8686
250	2.0	2			0.4397	0.7776	1.2173			0.5094	0.7724	1.2818		0.4007	0.6600	0.7517	1.8125	
250	2.0	3			0.4398	0.7786	1.2183			0.5107	0.7731	1.2837		0.4048	0.6613	0.7540	1.8201	
250	2.0	5			0.4371	0.7785	1.2155			0.5119	0.7733	1.2852		0.4051	0.6593	0.7558	1.8202	
250	2.0	10			0.4363	0.7788	1.2152			0.5117	0.7735	1.2852		0.1575	0.3857	0.6237	0.7572	1.9241
250	2.3	2			0.4387	0.7768	1.2155			0.5086	0.7721	1.2807		0.4020	0.6608	0.7547	1.8176	
250	2.3	3			0.4389	0.7770	1.2159			0.5094	0.7724	1.2818		0.4041	0.6618	0.7569	1.8228	
250	2.3	5			0.4378	0.7773	1.2151			0.5096	0.7724	1.2820		0.4059	0.6625	0.7572	1.8256	
250	2.3	10			0.4367	0.7776	1.2143			0.5102	0.7726	1.2828		0.3923	0.6445	0.7585	1.7953	
500	1.5	2			0.4451	0.7568	1.2019			0.5098	0.7629	1.2728		0.3971	0.6482	0.7265	1.7718	
500	1.5	3			0.4468	0.7604	1.2072			0.5153	0.7670	1.2823		0.4065	0.6515	0.7239	1.7819	
500	1.5	5			0.4395	0.7662	1.2057			0.5111	0.7718	1.2829		0.3881	0.6190	0.7268	1.7340	
500	1.5	10		0.0805	0.3011	0.7727	1.1543		0.1514	0.4111	0.7751	1.3376		0.1249	0.3033	0.5077	0.7314	1.6673
500	1.7	2			0.4426	0.7683	1.2109			0.5096	0.7694	1.2791		0.3968	0.6515	0.7328	1.7812	
500	1.7	3			0.4450	0.7713	1.2163			0.5141	0.7724	1.2865		0.4097	0.6551	0.7329	1.7977	
500	1.7	5			0.4410	0.7755	1.2164			0.5145	0.7739	1.2885		0.3932	0.6322	0.7364	1.7618	
500	1.7	10			0.3762	0.7781	1.1542			0.4765	0.7755	1.2520		0.1251	0.3165	0.5311	0.7421	1.7148
500	2.0	2			0.4409	0.7748	1.2158			0.5109	0.7732	1.2841		0.3990	0.6560	0.7407	1.7957	
500	2.0	3			0.4413	0.7774	1.2188			0.5132	0.7751	1.2883		0.4041	0.6588	0.7424	1.8053	
500	2.0	5			0.4397	0.7793	1.2190			0.5142	0.7753	1.2895		0.3981	0.6462	0.7468	1.7911	
500	2.0	10			0.4289	0.7794	1.2082			0.5093	0.7753	1.2846		0.1334	0.3391	0.5638	0.7509	1.7872
500	2.3	2			0.4405	0.7769	1.2174			0.5099	0.7725	1.2824		0.4005	0.6577	0.7456	1.8038	
500	2.3	3			0.4398	0.7787	1.2185			0.5127	0.7737	1.2865		0.4060	0.6596	0.7485	1.8140	
500	2.3	5			0.4376	0.7792	1.2167			0.5133	0.7740	1.2873		0.4029	0.6535	0.7523	1.8086	
500	2.3	10			0.4380	0.7793	1.2173			0.5137	0.7737	1.2874		0.1418	0.3582	0.5917	0.7546	1.8464
750	1.5	2			0.4479	0.7371	1.1850		0.2271	0.5077	0.77495	1.4842		0.3998	0.6412	0.7165	1.7575	
750	1.5	3			0.4510	0.7390	1.1900			0.5132	0.7534	1.2666		0.4024	0.6395	0.7128	1.7547	
750	1.5	5			0.4342	0.7472	1.1814			0.5016	0.7625	1.2640		0.1606	0.3719	0.5922	0.7145	1.8393
750	1.5	10	0.0136	0.0668	0.2842	0.7600	1.1247		0.1185	0.3483	0.7693	1.2361		0.0979	0.2574	0.4450	0.7206	1.5209
750	1.7	2			0.4457	0.7530	1.1987		0.2347	0.5089	0.7609	1.5045		0.3976	0.6454	0.7233	1.7663	
750	1.7	3			0.4483	0.7571	1.2054			0.5137	0.7647	1.2783		0.4034	0.6479	0.7218	1.7731	
750	1.7	5			0.4401	0.7637	1.2038			0.5107	0.7704	1.2811		0.1607	0.3772	0.6088	0.7256	1.8723
750	1.7	10	0.0848		0.3145	0.7717	1.1711		0.1546	0.4162	0.7740	1.3448		0.1024	0.2705	0.4685	0.7322	1.5736
750	2.0	2			0.4436	0.7658	1.2095			0.5094	0.7684	1.2777		0.3958	0.6503	0.7321	1.7783	
750	2.0	3			0.4446	0.7698	1.2144			0.5130	0.7718	1.2848		0.4073	0.6537	0.7321	1.7931	
750	2.0	5			0.4418	0.7748	1.2166			0.5134	0.7740	1.2874		0.1614	0.3871	0.6268	0.7370	1.9124
750	2.0	10			0.3911	0.7775	1.1686			0.4854	0.7747	1.2601						

B	10^{-3}	10^{-2}	10^{-1}	1	Σ	10^{-3}	10^{-2}	10^{-1}	1	Σ	10^{-3}	10^{-2}	10^{-1}	1	Σ
1			0.3854	0.6075	0.9928			0.3894	0.6331	1.0225	0.2334	0.3859	0.6671	0.6744	1.9608
2			0.4628	0.6486	1.1114			0.5123	0.6321	1.1445	0.2937	0.4894	0.6610	0.6728	2.1168
5		0.0336	0.3941	0.6136	1.0413			0.4352	0.6180	1.0532	0.4011	0.5860	0.6744	0.6789	2.3405
10			0.4570	0.6392	1.0962			0.4987	0.6243	1.1230	0.0428	0.3809	0.6074	0.6499	1.6810
25		0.0292	0.4067	0.6200	1.0559			0.4803	0.6386	1.1189	0.0666	0.2911	0.6165	0.6551	1.6293
100			0.4809	0.6532	1.1342			0.4976	0.6288	1.1264	0.1803	0.3756	0.5711	0.5755	1.7025

(a) SoftMax

(b) Garbage

(c) EOS

Table 9: PROSER* PARAMETER OPTIMIZATION ON P_1 .

B	10^{-3}	10^{-2}	10^{-1}	1	Σ	10^{-3}	10^{-2}	10^{-1}	1	Σ	10^{-3}	10^{-2}	10^{-1}	1	Σ
1	0.0284	0.1282	0.3846	0.6899	1.2310	0.0537	0.2339	0.5101	0.6669	1.4647	0.0662	0.3113	0.5759	0.6491	1.6024
2	0.0284	0.1355	0.3713	0.6912	1.2263	0.0590	0.2349	0.4993	0.6700	1.4632	0.0538	0.2569	0.5534	0.6406	1.5048
5	0.0233	0.1071	0.3587	0.6923	1.1813	0.0570	0.2483	0.5033	0.6775	1.4862		0.3169	0.5739	0.6495	1.5403
10	0.0206	0.1026	0.3364	0.6895	1.1491	0.0745	0.2294	0.4976	0.6773	1.4788	0.0911	0.3270	0.5717	0.6523	1.6420
25	0.0203	0.0962	0.3393	0.6945	1.1503	0.0504	0.2283	0.4938	0.6712	1.4437		0.3210	0.5880	0.6571	1.5662
100	0.0145	0.0825	0.3415	0.6910	1.1296	0.0594	0.2208	0.5017	0.6766	1.4585	0.0545	0.3000	0.5850	0.6552	1.5947

(a) SoftMax

(b) Garbage

(c) EOS

Table 10: PROSER* PARAMETER OPTIMIZATION ON P_2 .

B	10^{-3}	10^{-2}	10^{-1}	1	Σ	10^{-3}	10^{-2}	10^{-1}	1	Σ	10^{-3}	10^{-2}	10^{-1}	1	Σ
1		0.1472	0.4228	0.7466	1.3166		0.2725	0.5505	0.7455	1.5686			0.4485	0.6855	1.1340
2		0.1446	0.4342	0.7500	1.3288		0.2881	0.5722	0.7583	1.6186		0.2211	0.6056	0.7380	1.5647
5		0.1430	0.4267	0.7451	1.3148		0.2813	0.5610	0.7471	1.5894		0.2963	0.6431	0.7584	1.6977
10		0.1545	0.4387	0.7524	1.3456	0.1143	0.2967	0.5746	0.7539	1.7394		0.1730	0.6240	0.7499	1.5469
25		0.1506	0.4259	0.7465	1.3230	0.1079	0.2918	0.5654	0.7464	1.7115			0.6110	0.7430	1.3539
100		0.1494	0.4271	0.7453	1.3218	0.1175	0.2864	0.5629	0.7478	1.7145			0.3251	0.6390	0.7585

(a) SoftMax

(b) Garbage

(c) EOS

Table 11: PROSER* PARAMETER OPTIMIZATION ON P_3 .